Nature Communications

https://doi.org/10.1038/s41467-026-70526-9

Article in Press

Endogenous VEGF signaling acts as a guardian of human primed pluripotency

Received: 30 April 2025

Accepted: 1 March 2026

Cite this article as: Wu, X., Wen, C., Zhu, C. *et al.* Endogenous VEGF signaling acts as a guardian of human primed pluripotency. *Nat Commun* (2026). https://doi.org/10.1038/s41467-026-70526-9

Xu Wu, Chunsheng Wen, Chaonan Zhu, Huiyuan Jiao, Chenge Xin, Haokun Jiang, Ran Tong, Yuwei Huang, Liyun Yuan, Min Shao, Hanzhi Zhao, Junjie Gu, Qiong Wu, Feng Zhang, Han Wang, Yifan Zhou, Bing Liao, Lingjie Li, Ying Jin & Hui Li

Endogenous VEGF signaling acts as a guardian of human primed pluripotency

Xu Wu[1,#], Chunsheng Wen[2,#], Chaonan Zhu[1,#], Huiyuan Jiao[1], Chenge Xin[1], Haokun Jiang[1], Ran Tong[1], Yuwei Huang[3], Liyun Yuan[3], Min Shao[2], Hanzhi Zhao[2], Junjie Gu[1], Qiong Wu[1], Feng Zhang[1], Han Wang[1], Yifan Zhou[2], Bing Liao[1], Lingjie Li[1], Ying Jin[1,2,*], Hui Li[1,*]

[1]Department of Histoembryology, Genetics and Developmental Biology, Shanghai Key Laboratory of Reproductive Medicine, Shanghai Jiao Tong University School of Medicine, Shanghai, 200025, China

[2]CAS Key Laboratory of Tissue Microenvironment and Tumor, Shanghai Institute of Nutrition and Health (SINH), Chinese Academy of Sciences (CAS), Shanghai, 200031, China

[3]Bio-Med Big Data Center, CAS Key Laboratory of Computational Biology, Shanghai Institute of Nutrition and Health, Chinese Academy of Sciences, Shanghai, 200031, China

[#] These authors contributed equally to this work.

* Correspondence: yjin@sibs.ac.cn; lihuilh@shsmu.edu.cn

Summary

The maintenance of human embryonic stem cell (hESC) self-renewal and pluripotency is governed by distinct signaling pathways, yet endogenous pluripotency-supporting pathways remain understudied despite extensive exogenous signaling research. Here, we identify a previously unrecognized role of endogenous VEGF signaling in sustaining primed hESC pluripotency. VEGF signaling is robustly actived in primed hESCs, quiescent in naïve cells, and inactivated upon differentiation. Strikingly, targeted VEGF inhibition (pharmacological, soluble decoy receptors [sFLT1/sKDR], or CRISPR-mediated VEGFR1/2 knockout) in primed hESCs disrupts self-renewal and induces trophoblast-like differentiation. Mechanistically, VEGF inhibition activates the BMP pathway and downregulates NANOG, which directly binds and represses select BMP components and trophoblast lineage-specific genes. Functionally, BMP inhibition partially and NANOG overexpression substantially rescue the phenotype induced by VEGF signaling ablation. Collectively, our work uncovers a pivotal VEGF-dependent network maintaining primed pluripotency, providing valuable insights into integrated pluripotency and lineage regulation by signaling cascades and transcription factors.

Introduction

During mammalian embryogenesis, transient pluripotent cell populations, such as those in the inner cell mass (ICM) and epiblast, arise within blastocysts. These cells give rise to all somatic and germ cells in mammals and serve as the foundation for embryonic stem cells (ESCs) *in vitro*[1-3]. Human ESCs possess the capacity of unlimited self-renewal and the potential of differentiation into all cell types of the body. These unique features make them a powerful tool for modeling early embryonic development and human diseases, also offering the great potential for disease treatment. However, challenges remain in generating hESCs with high quality and functional cells with high efficiency. A thorough understanding of the regulatory mechanisms governing hESC pluripotency and fate decision is thus essential. Currently, pluripotency has been categorized into two main

states, naïve and primed. The pluripotent cells in the ICM and pre-implantation epiblasts (pre-EPI) are considered to be naïve, while the cells in the post-implantation epiblasts (post-EPI) are thought to be primed[4]. As to *in vitro* cultured pluripotent stem cells (PSCs), mouse ESCs (mESCs) exhibit features of naïve pluripotency, whereas routinely cultured human ESCs (hESCs) display characteristics of primed pluripotency, similar to mouse epiblast stem cells (mEpiSCs)[4-6]. Pluripotency and unlimited self-renewal, the two hallmarks of hESCs, are governed by both intrinsic factors and extrinsic signaling pathways. Transcriptional factors (OCT4, SOX2, and NANOG) form a core regulatory hub in hESCs, interacting with each other and co-occupying their regulatory regions to create autoregulatory loops that stabilize their expression[7, 8]. They also jointly regulate a network of other transcription factors and key genes crucial for maintaining hESC identity[7, 8]. Additionally, they control the expression of differentiation-associated genes, thereby modulating lineage commitment[9]. However, phenotypic outcomes of their absence in hESCs are not entirely consistent across studies, likely due to variations in the cell lines and culture conditions applied in different studies. For example, *NANOG* deficiency was reported to lead to neuroectodermal differentiation or differentiation towards trophectoderm or primitive endoderm[10-14]. Currently, our understanding of how NANOG safeguards hESC identity is far from complete.

Extrinsic signaling circuitries triggered by growth factors are also critical for hESC maintenance. A precise combination of growth factors, including bFGF, TGF-β/ACTIVIN/NODAL, and INSULIN/IGF, is essential for activating the core transcriptional circuitry and preventing differentiation in hESCs[15-20]. Among these factors, bFGF activates the MAPK/ERK1/2 pathway, enhancing the self-renewal-related gene expression[21]. Although excessive ERK1/2 activation can induce differentiation, bFGF also engages the PI3K pathway, which counteracts ERK overactivation and maintains hESC self-renewal. In contrast to the extensive research on exogenous factors, roles of endogenous molecules in hESC fate decisions remain poorly explored. It was reported

that ELABELA, an endogenous peptide hormone, promotes hESC self-renewal by activating the PI3K/AKT pathway[22]. Further exploration of endogenous signaling pathways important for hESC fate decision is necessary to deepen our understanding of early human embryonic development and optimize the hESC culture system.

The vascular endothelial growth factor (VEGF) signaling pathway is well known for its vital roles in vasculogenesis, angiogenesis, and lymphangiogenesis[23]. However, its role in early human development during the peri-implantation period has not been documented. Among VEGF ligands (VEGFA, VEGFB, VEGFC, VEGFD, and placental growth factor, PlGF), VEGFA, originally known as VEGF, is the most studied. These VEGF ligands bind to transmembrane receptor tyrosine kinases (VEGFR1/FLT1, VEGFR2/KDR/FLK1, and VEGFR3/FLT4) with varying specificity and distinct functional roles[24]. VEGF signaling has been implicated in hESC differentiation processes, such as mesendodermal and mesodermal endothelium differentiation[25-27]. In mESCs, VEGF signaling is quiescent under normal conditions, but prolonged culture, even in LIF-supplemented medium, induces spontaneous VEGF secretion and differentiation towards meso-endoderm lineages[28]. However, the activity and function of VEGF signaling in hESCs remain unclear.

In this study, we screened a panel of small molecules to identify additional signaling pathways required for identity maintenance of primed hESCs and discovered that endogenous VEGF signaling was indispensable for maintaining primed pluripotency and blocking trophoblast differentiation in primed hESCs. Our results demonstrated that these functions were mediated through activating NANOG expression and concurrent suppressing the BMP signaling pathway. Our findings provide valuable insights into how cell fate decision is regulated through interplay between signaling pathways and transcriptional regulation in human PSCs.

Results

Unique activation of endogenous VEGF signaling in primed hESCs

Receptor tyrosine kinases (RTKs) mediate cellular responses to a wide range of signals. However, their roles in maintaining hESC self-renewal and pluripotency remain poorly characterized. To address this, we screened a panel of small-molecule inhibitors targeting RTKs including those for EGF (epidermal growth factor), VEGF, and PDGF (platelet-derived growth factor). We used the primed SHhES8 hESC line, which was derived and characterized in our lab[29], throughout the study, unless otherwise indicated. Remarkably, hESCs treated with VEGFR inhibitor Axitinib (Axi) for 2 days exhibited the morphology of extensive and uniform differentiation, accompanied by a moderate level of cell death (Fig. 1a). In contrast, inhibition of PDGFR failed to induce significant morphological changes. Similarly, inhibition of EGFR, despite triggering marked cell death, did not elicit discernible differentiation phenotype. To verify the specificity of VEGFR inhibition, we treated hESCs with two additional pan-VEGFR inhibitors, Tivozanib (Tiv) and Lenvatinib (Len). Both of them induced a comparable differentiation phenotype, yet caused noticeably less cell death and yielded a more synchronous change in the morphology than Axi (Supplementary Fig. 1a). The efficacy of these inhibitors was determined by western blot analysis of levels of phospho-ERK1/2 (T202/Y204) and phospho-AKT (S473) (Supplementary Fig. 1b-c), common downstream effectors of RTKs. The results showed that all three VEGFR inhibitors markedly reduced the phosphorylation levels of ERK1/2 and AKT. In contrast, EGFR inhibition exerted a modest effect on the phosphorylation of these kinases, while PDGFR inhibition failed to decrease phosphorylation of ERK1/2 or AKT, likely due to low basal PDGF pathway activity in hESCs (Supplementary Fig. 1d). These findings indicate that VEGF signaling might play an important role in maintaining the undifferentiated state of primed hESCs.

Given that our culture medium lacked exogenous VEGF ligands, we next examined the expression and activity of VEGF signaling components in hESCs. Real-time quantitative PCR (RT-qPCR) analyses revealed higher levels of *VEGFR1*, *VEGFR2*, *VEGFA*, and *VEGFB* in undifferentiated hESCs (Fig. 1b). Similar expression patterns

were observed in two additional primed hESC lines, H9 and H1 (Supplementary Fig. 1e, f). Notably, highly expressed VEGF signaling components were markedly down-regulated upon differentiation induced by the E6 medium, in a manner similar to the down-regulation of core pluripotency factors (Fig. 1b). Differentiation was indicated by the down-regulation of pluripotency factors (*OCT4*, *NANOG*) and up-regulation of lineage-specific markers (*PAX6*, *T* and *GATA3*) (Fig. 1b). Consistently, our immunofluorescence staining results further showed that VEGF ligands (VEGFA and VEGFB) and receptors (VEGFR1 and VEGFR2) were robustly expressed in primed hESCs, and that their levels decreased shortly after differentiation (Fig. 1c). Moreover, VEGFR1 and VEGFR2 were down-regulated upon differentiation induced by either retinoic acid (RA) treatment (Supplementary Fig. 1g-i) or embryoid body (EB) formation (Supplementary Fig. 1j-l). These results indicate that primed hESCs produce high levels of VEGF signaling components, and their expression is tightly linked to hESC undifferentiated state.

Since primed and naïve hESCs rely on distinct signaling for pluripotency maintenance, we compared the expression pattern of VEGF signaling components between these two pluripotency states. We converted primed hESCs to the naïve state via the 5i/L/FA conversion protocol[30 31](Fig. 1d). Intriguingly, high levels of *VEGFR1* and *VEGFR2* were uniquely detected in primed hESCs, but not in naïve hESCs, whereas hESCs at both states expressed abundant *VEGFA* and *VEGFB* ligands (Fig. 1e). It is known that VEGF signaling activation is initiated by ligand binding to receptors, which then dimerize and phosphorylate intracellular tyrosine residues[24, 32]. To assess VEGF signaling activity in cells at different states, we examined levels of VEGFR1/2 and their phosphorylation in naïve and primed hESCs as well as E6-induced differentiated cells for hESC lines SHhES8 and H9 cells. Our results showed that both VEGFR1 and VEGFR2 were activated in primed hESCs cultured in the mTeSR1 medium, whereas their activation was absent in naïve hESCs and reduced in differentiated cells (Fig. 1f, g). Collectively,

these findings demonstrate that endogenous VEGF signaling is specifically activated in primed hESCs and silenced in naïve hESCs.

Essential roles of VEGF signaling in maintaining self-renewal and preventing trophoblast differentiation

To characterize the function of VEGF signaling in hESCs, we inhibited this pathway using two pan-VEGFR inhibitors, Tiv and Len. Compared with DMSO-treated controls, hESC colonies treated with either inhibitor exhibited loosened morphology within 24 hours (h), followed by flattening of cells at the colony periphery and significant cell death by 48 h. Strikingly, all cells differentiated with a uniform cobblestone-like morphology by day 3 (Fig. 2a). Our western blot analysis showed decreases in levels of phosphorylated VEGFR1 and VEGFR2 (pVEGFR1 and pVEGFR2), validating the efficient inactivation of VEGF signaling (Fig. 2b, c) by the inhibitor. Moreover, RT-qPCR analysis revealed significant down-regulation of pluripotency genes and robust up-regulation of trophoblast markers in inhibitor-treated cells, with no or limited changes in markers of the three germ layers (ectoderm, mesoderm, and endoderm) (Fig. 2d). Similar results were obtained in H1 hESCs, ruling out cell line-specific effects (Supplementary Fig. 2a, b) Moreover, our immunofluorescence staining results illustrated the loss of OCT4 as well as drastic induction of trophoblast markers GATA3 and KRT7 induced by VEGFR inhibition (Supplementary Fig. 2c). Thus, VEGF signaling inhibition disrupts self-renewal in primed hESCs and induces differentiation towards the trophoblast lineage.

To address potential off-target effects of small molecules, we generated a hESC line with doxycycline (DOX)-inducible overexpression (OE) of soluble VEGF receptors *sFLT1* and *sKDR*. These soluble receptors lack intracellular domains and act as decoy receptors for VEGF ligands. Two clones (referred to as SS iOE #7 and #10 thereafter) were selected and used in subsequent experiments. Serving as a negative control, a control hESC line transfected with an empty vector (Flag iOE) was also generated. After 6 days of DOX treatment, robust induction of *sFLT1* and *sKDR* was observed in cells of both selected

clones, leading to a significant reduction in levels of pVEGFR1 and pVEGFR2 (Fig. 2e-g). Morphological changes indicative of differentiation were observed in DOX-treated SS iOE cells but not in control cells (Fig. 2h). Moreover, RT-qPCR results showed down-regulation of pluripotency markers and up-regulation of trophoblast markers in DOX-treated SS iOE #7 and SS iOE #10 cells compared with untreated counterparts and Flag iOE control cells (Fig. 2i). Furthermore, immunofluorescence staining detected the loss of OCT4 and induction of GATA3 in DOX-treated SS iOE cells (Supplementary Fig. 2d). Therefore, like small molecule inhibitors, enforced expression of soluble VEGF receptors drives primed hESCs to exit the self-renewal state and initiate differentiation towards the trophoblast lineage.

To further validate these findings, we established inducible *VEGFR1* and *VEGFR2* double knockout (dKO) hESCs using the CRISPR-Cas9 genome editing strategy with a modified protocol [33]. The successful dKO was verified by RT-qPCR and western blot analyses (Supplementary Fig. 3a-c). As expected, dKO cells exhibited the differentiated morphology and induction of trophoblast markers (Supplementary Fig. 3d-f), consistent with phenotypes observed in cells treated with VEGFR inhibitors or cells with soluble VEGFR OE. Together, these results obtained from experiments with three loss of function approaches robustly demonstrate the essential role of the VEGF signaling in the maintenance of self-renewal and highlight its importance in repressing trophoblast lineage specification in primed hESCs.

Given that VEGF signaling inhibition robustly activated the trophoblast program in hESCs, we next sought to determine the functional consequences of activating VEGF signaling during trophoblast differentiation. To this end, we established a hESC line with DOX-inducible OE of VEGFA165 (referred to as VEGFA165 iOE thereafter)[25], the predominant VEGF isoform. After DOX-induced *VEGFA165* OE in hESCs was validated (Supplementary Fig. 3g), edited cells were cultured in the BAP medium, a well-established condition for inducing trophoblast-like cells from hESCs[34], with or without

DOX for 1 day (Supplementary Fig. 3h). As anticipated, trophoblast genes were efficiently induced by the BAP medium. However, the induction of trophoblast morphology and marker gene expression was evidently suppressed by VEGFA165 OE (Supplementary Fig. 3i, j). Our results indicate that enforced VEGFA165 expression represses trophoblast induction in primed hESCs.

VEGF signaling inhibits BMP pathway activity to block trophoblast induction

To elucidate how VEGF signaling sustained hESC self-renewal and repressed trophoblast lineage specification, genome-wide transcriptional profiles were analyzed by RNA-sequencing (RNA-seq) on hESCs treated with a VEGFR inhibitor or OE of soluble VEGF receptors at multiple time points : Len or Tiv for 3h, 6h, 12h and 18h; Len or Axi for D1, D2 and D3; SS iOE#10 for D0, D1, D2 and D6. Among these samples, inhibitor-treated cells at day 3 and DOX-induced SS iOE cells at day 6 contained the most abundant numbers of differentially expressed genes (DEGs, two-fold change and FDR-adjusted *p*-value < 0.05) (treatment vs control), with 4125 and 5484 DEGs, respectively. Given that VEGF signaling inhibition activated a trophoblast-like transcriptional program, we analyzed up-regulated DEGs in these samples using the Metascape (http://metascape.org), a web-based tool for enrichment analysis. Terms associated with stem cell differentiation and placenta development were enriched (Fig. 3a, b), in accordance with the phenotypic changes observed following VEGF signaling inactivation in primed hESCs. Notably, enriched terms included SMAD protein signal transduction and BMP signaling pathway known to be closely linked to trophoblast and placenta development. Gene Set Enrichment Analysis (GSEA) further validated the enrichment of the BMP pathway in these up-regulated DEGs (Fig. 3c, d). A heatmap illustrated the progressive induction of BMP pathway members following VEGF signaling inactivation (Supplementary Fig. 4a, b), consistent with the outcomes of our GSEA. To experimentally validate activated BMP signaling after VEGF signaling inactivation, we assessed the kinetics of BMP4 pathway activity by measuring the phosphorylation levels of its

downstream effectors SMAD1/5/8 in cells treated with DMSO or inhibitors (Tiv and Len) and in SS iOE cells with or without DOX treatment. Our result showed drastic increases in the levels of phosphorylated SMAD1/5/8 at 4 h of the inhibitor treatment (Fig. 3e, f), and at day 6 of the DOX addition in SS iOE cells, although DOX did not alter levels of phosphorylated SMAD1/5/8 in control cells (Fig. 3g, h).

To determine whether elevated BMP pathway would play a pivotal role in trophoblast differentiation triggered by VEGF signaling inactivation, we employed two BMP type I receptor kinase inhibitors (LDN-214117 and DMH1). Consistently, VEGFR inhibitor treatment (Tiv and Len) or OE of soluble receptors down-regulated pluripotency genes and up-regulated trophoblast markers significantly (Fig. 3i, j), accompanied by cell morphological changes (Supplementary Fig. 4c, d). Notably, BMP inhibitors (LDN-214117 or DMH1) suppressed the up-regulation of trophoblast genes and morphological changes caused by VEGF signaling inactivation. However, BMP inhibitor treatment did not rescue the down-regulation of pluripotency genes (Fig. 3i, j). The inhibitory effects of LDN-214117 or DMH1 on SMAD1/5/8 phosphorylation were validated (Supplementary Fig. 4e-h). These results lead to our conclusion that endogenous VEGF signaling suppresses the BMP pathway to block trophoblast differentiation in primed hESCs.

VEGF signaling sustains NANOG expression and pluripotency

As mentioned above, inhibition of the BMP pathway efficiently blocked VEGF signaling inactivation-induced trophoblast differentiation in hESCs, but could not restore the expression of pluripotency factors. This observation suggested that VEGF signaling might modulate additional factors to preserve hESC identity. To identify such factors, we analyzed down-regulated DEGs in VEGFR inhibitor-treated cells at day 3 and in DOX-treated SS iOE cells at day 6. As expected, terms associated with negative regulation of cell differentiation were enriched in these DEGs (Fig. 4a, b), in line with the observed differentiation phenotype following VEGF signaling depletion in hESCs. Of note, terms related to OCT4, SOX2, NANOG and positive regulation of DNA-binding transcription

factor activity were also enriched. Consistently, our heatmap illustrated a decline in the expression of pluripotency-associated genes, with *NANOG* exhibiting a particularly pronounced and rapid reduction in VEGFR inhibitor-treated cells (Supplementary Fig. 5a, b). Similar results were obtained in SS iOE cells after DOX treatment (Supplementary Fig. 5c). The down-regulation of NANOG and OCT4 in response to VEGF signaling inactivation was further validated at a protein level (Fig. 4c-f and Supplementary Fig. 5d-g).

Based on the observation that NANOG levels decreased most rapidly and dramatically among the down-regulated pluripotency factors, we investigated whether VEGF signaling pathway ensures hESC self-renewal and pluripotency by maintaining NANOG expression. To this end, we generated a DOX-inducible *NANOG* OE hESC line (referred to as NANOG iOE thereafter). The efficient induction of *NANOG* OE by DOX was verified (Fig. 4g-i). Functionally, *NANOG* OE substantially diminished the elevation of trophoblast-specific genes and SMAD1/5/8 phosphorylation levels, as well as morphological alterations caused by the VEGFR inhibitor (Fig. 4g-i and Supplementary Fig. 5h). The decrease in pluripotency gene expression was also partially corrected (Fig. 4g). As a negative control, DOX treatment did not provoke any of these responses in wild-type hESCs (Fig. 4h, i and Supplementary Fig. 5i), verifying that *NANOG* OE was responsible for the rescue effect in *NANOG* iOE cells. These results demonstrated the capacity of NANOG to counteract differentiation phenotypes induced by VEGF signaling inactivation. To further characterize the role of NANOG in VEGF signaling-mediated functions, we generated a DOX-inducible NANOG OE hESC line in SS iOE #10 cells (referred to as SSN iOE thereafter). In this cell line, the addition of DOX simultaneously induces OE of *NANOG* as well as two soluble VEGF receptors. Using both SS iOE and SSN iOE cell lines, we showed that *NANOG* OE largely rescued down-regulation of pluripotency genes, up-regulation of trophoblast genes and elevations in the level of SMAD1/5/8 phosphorylation, as well as morphological changes triggered by OE of

soluble VEGF receptors (Fig. 4j-l and Supplementary Fig. 5j). Collectively, these results support the conclusion that NANOG functions as a key effector downstream of the VEGF signaling pathway to maintain hESCs in an undifferentiated and primed pluripotency state, although we did not find a direct link between VEGF signaling and *NANOG* transcription in hESCs.

NANOG directly regulates BMP signaling and trophoblast genes

To elucidate how NANOG functions downstream of the VEGF signaling pathway, we performed RNA-seq analyses on cells from the following 3 groups: NANOG iOE, SS iOE and SSN iOE, with indicated treatments (Fig. 5a, b). We analyzed DEGs that were altered by the VEGFR inhibitor or the soluble VEGFR OE and subsequently rescued by concurrent *NANOG* OE (with fold change > 2 or < 0.5 and FDR-adjusted *p*-value < 0.05). In *NANOG* iOE cells treated with the VEGFR inhibitor, we identified 202 such DEGs, including 29 down-regulated genes rescued by *NANOG* OE (referred to as NANOG_iOE_down_rescued) and 173 up-regulated genes rescued by NANOG OE (referred to as NANOG_iOE_up_rescued). Moreover, in SS iOE and SSN iOE cells, we detected 863 DEGs, comprising of 499 down-regulated genes rescued by NANOG OE (referred to as SSN_iOE_down_rescued) and 364 up-regulated genes rescued by NANOG OE (referred to as SSN_iOE_up_rescued) (Supplementary Fig. 6a). Our hierarchical clustering analysis revealed that *NANOG* OE rescued a subset of pluripotency genes down-regulated by VEGF signaling inactivation (e.g., *NODAL*, *DPPA4*, *PRDM14*, *LEFTY1*, and *OCT4*) and trophoblast genes up-regulated by VEGF signaling inactivation (e.g., *BMP2*, *BMP4*, *BMP5*, *BMP7*, *GATA2*, *GATA3*, and *KRT7*) (Fig. 5a, b). Using Metascape, we conducted enrichment analysis for DEGs down-regulated by VEGF signaling inactivation and rescued by *NANOG* OE in both VEGF signaling inactivation strategies (inhibitor treatment and soluble receptor OE). Enriched terms included signaling pathways regulating pluripotency of stem cells, transcriptional regulation of pluripotency stem cells, and OCT4, SOX2, NANOG activated genes related to

proliferation, in accordance with the central role of NANOG in hESC pluripotency maintenance (Fig. 5c, d). Notably, for DEGs up-regulated by VEGF signaling inactivation and rescued by *NANOG* OE terms related to the BMP signaling pathway, stem cell differentiation, and embryonic placenta development were enriched (Fig. 5e, f). These analyses supported the notion that NANOG could mediate the function of VEGF signaling by sustaining pluripotency gene expression as well as suppressing the BMP pathway and trophoblast differentiation. Further examination of DEGs of NANOG_iOE_up_rescued and SSN_iOE_up_rescued identified a set of BMP pathway genes (Supplementary Fig. 6b, c). Interestingly, some genes in this set were shown to be up-regulated in inducible *NANOG* knockout (KO) hESCs (RNA-seq data from our lab[35]), corroborating a suppressive effect of NANOG on BMP pathway transcripts (Supplementary Fig. 6d). These data strongly demonstrate that NANOG is a key player downstream of VEGF signaling for sustaining pluripotency gene expression as well as repressing the expression of certain BMP signaling components and trophoblast genes in primed hESCs.

To determine whether NANOG could directly bind to the genomic loci of BMP pathway members, we analyzed NANOG chromatin immunoprecipitation sequencing (ChIP-seq) data (data from our lab[35]). Chromatin-state annotations were generated using ChromHMM based on ENCODE data[36, 37]. We found that NANOG bound to the promoter or enhancer regions of certain BMP pathway genes (Fig. 5g) and key trophoblast markers, such as *GATA3*, *CDX2*, *TP63*, *TFAP2A* and *TEAD1* (Fig. 5h). The deposition of NANOG on these regions was validated by our ChIP-qPCR analyses (Fig. 5i, j). These data indicate that NANOG safeguards human primed pluripotency through both activating of pluripotency-associated genes and suppressing differentiation-associated genes (e.g. BMP pathway components and trophoblast lineage genes). Nevertheless, the underlying mechanisms through which NANOG fulfills its dual regulatory function in gene expression remain incompletely understood.

In addition, we found that NANOG occupied an enhancer within the gene body of

VEGFR1 and a weak enhancer located 7 kb upstream of *VEGFR2* (Supplementary Fig. 6e), as verified by our ChIP-qPCR assays (Supplementary Fig. 6f). To test whether NANOG could control the expression of VEGF receptors, we examined their transcript levels in *NANOG* iKO (Supplementary Fig. 6g) and *NANOG* iKD (Supplementary Fig. 6h) hESCs. *NANOG* depletion significantly downregulated *VEGFR2*, while the *VEGFR1* transcript level was not significantly changed, indicating distinct regulatory mechanisms for these two receptors. The reciprocal regulation between NANOG and VEGF signaling highlights mutually reinforcing positive feedback loops between transcription factors and signaling pathways that safeguard hESC self-renewal and pluripotency.

VEGF signaling inhibition activates a trophoblast-like transcriptional program

As the treatment of primed hESCs with VEGFR inhibitors (Tiv and Len) robustly activated trophoblast genes and induced uniform morphological changes (Fig. 6a), we further characterized the properties of these differentiated cells. Initially, we assessed the expression of HLA-ABC, a marker known to be present in hESCs but absent in trophoblast-like cells, mononuclear trophoblast marker GATA3, and trophectoderm (TE) cell surface marker TROP2 (also known as TACSTD2) in hESCs cultured in the self-renewal supporting mTeSR1 medium and treated with VEGFR inhibitors (Tiv or Len) for 3 or 5 days. Our flow cytometric analyses revealed that nearly all differentiated cells expressed GATA3 and TROP2, whereas the majority did not express HLA-ABC. Conversely, undifferentiated hESCs showed the opposite pattern (Fig. 6b, c). These findings suggested that the loss of VEGF signaling activity caused hESCs to exit the pluripotency state and undergo differentiation towards the extra-embryonic trophoblast lineage. We then examined the *ELF5* promoter, which is known to be specifically hypomethylated in trophoblast cells[38]. We found that the hypermethylated state of the *ELF5* promoter in untreated hESCs was switched to a hypomethylated state following the inhibitor treatment (Fig. 6d), indicating an epigenetic reprogramming accompanied with the cell fate change. These results indicate that the VEGFR inhibition induces nearly

homogeneous trophoblast-like differentiation.

Human placenta comprises three main trophoblast subpopulations: cytotrophoblast (CT), extravillous trophoblast (EVT), and syncytiotrophoblast (ST). CT cells are *in vivo* counterparts of *in vitro* human trophoblast stem cells (hTSCs) and can differentiate into the other two differentiated cell types. Hence, we examined the expression of specific markers in Tiv or Len-treated cells and found that the inhibitor treatment robustly activated markers characteristic of CT cells, with mild effects on the expression of EVT and ST markers (Fig. 6e). At the protein level, immunofluorescence staining further illustrated the universal expression of CDX2, ELF5, and TP63, which are indicative of trophectoderm or CT cells, in inhibitor-treated cells (Fig. 6f). Therefore, these inhibitor-treated cells appear to acquire several features of the trophectoderm or CT. To test whether these cells would possess the capacity to differentiate towards EVT and ST trophoblast subtypes, we employed a previously published method[39]. When being cultured in the medium designed to induce EVT or ST differentiation, the inhibitor-treated cells expressed EVT-specific genes (*ITGA1*, and *PECAM1*) and ST-specific genes (*hCGA*, *hCGB*, and *PSG9*) (Fig. 6g). Nevertheless, these cells failed to propagate in self-renewal culture conditions, indicating a lack of intrinsic self-renewal capacity. Finally, given that trophoblast and amnion share certain genes, such as *GATA3* and *KRT7*, we examined the expression of a set of genes, including *ACMSD*, *AQP9*, *CLDN22*, *TMEM174*, *MCCD1*, *HBA1*, and *SOX11*, which have been reported to be highly and specifically expressed in the amnion[40]. Based on our RNA-seq data, these genes were not upregulated in VEGF signaling deficiency-induced differentiated cells (Fig. 6h). These findings once again indicate that the endogenous VEGF signaling pathway safeguards the primed pluripotency of hESCs. The loss of VEGF signaling activity results in hESCs to exit from the primed pluripotency state and differentiate into trophoblast-like cells.

Discussion

We here report a previously unrecognized role of endogenous VEGF signaling in safeguarding human primed pluripotency (Fig. 7). We found that i) VEGF signaling is specifically and robustly activated in primed hESCs, but is silent in naïve hESCs; ii) In primed hESCs, VEGF signaling inhibition disrupts self-renewal and activates a trophoblast-like transcriptional program, whereas its overactivation impedes this inductive process. These results demonstrate that the endogenous VEGF signaling is essential for maintaining self-renewal and pluripotency in primed hESCs. Mechanistically, we elucidate that VEGF signaling suppresses the BMP pathway and activates the expression of NANOG, which, in turn, directly represses the expression of BMP pathway components/trophoblast-associated genes and sustains the expression of pluripotency genes. Therefore, this study uncovers an additional and critical signaling pathway governing cell fate determination of hESCs, shedding fresh lights on the interplay between the signaling pathway and transcription factor in the maintenance of human primed pluripotency.

One of our interesting findings is distinct expression patterns of VEGF signaling components in naïve and primed hESCs, which represent pre-implantation and post-implantation pluripotent cells, respectively. We found that the VEGF pathway was robustly active in primed hESCs, while it was quiencent in naïve hESCs. This is consistent with a study of 3D-cultured human pre-gastrulation embryos, which identified VEGF signaling pathway genes in the post-EPI state, but not in the ICM or pre-EPI. Notably, immunostaining data from this study showed that VEGFR2 (also known as KDR), used as a marker for extra-embryonic mesoderm, was highly co-expressed with OCT4 within the epiblasts of 3D-cultured embryos at the 14-day post-fertilization stage[41]. Moreover, spatial profiling of early non-human primate (common marmoset) gastrulation in utero revealed *VEGFR2* expression in the pluripotent embryonic disc at Carnegie stages (CS) 5 and 6[42]. These findings indicate that the expression of VEGF receptors is pluripotency state dependent both in *in vitro* cultured pluripotent stem cells and in primate early

embryos *in vivo*. Consistent with the high activity of VEGF signaling in primed hESCs, its ablation severely disrupted self-renewal and robustly induced extra-embryonic lineage specification. Whether VEGF signaling exerts a pluripotency stage-specific role during the naïve-to-primed transition of hESCs, and whether its inhibition can promote primed-to-naïve conversion or sustain long-term naïve pluripotency, warrants further investigation. Additionally, physiological roles of VEGF signaling in early human embryonic development, particularly in embryonic implantation, remain poorly characterized.

The FGF signaling pathway, a well-established RTK signaling essential for primed hESC pluripotency, shares downstream branches such as MEK/ERK and PI3K/AKT with the VEGF pathway. Given that both FGFR and MEK inhibitors could induce trophoblast marker expression[43, 44], we propose that the VEGF and FGF pathways converge on the MEK/ERK cascade to sustain hESC pluripotency. Our findings demonstrate that VEGF pathway inactivation disrupted primed hESC self-renewal even in the mTeSR1 medium supplemented with FGF, suggesting that exogenous bFGF supplemented in the medium could not replace endogenous VEGF signaling. Moreover, VEGF inhibitors not only triggered trophoblast-like lineage specification but also led to cell death, which is likely associated with the cell survival-linked PI3K/AKT branch. The shared and distinct roles of the FGF and VEGF signaling pathways in sustaining human primed pluripotency represent an intriguing research focus that merits in-depth exploration.

Mechanistically, VEGF signaling secures human primed pluripotency through sustaining NANOG expression and suppressing BMP signaling. Our results showed that the increase in pSMAD1/5/8 levels and the decrease in NANOG expression both occurred rapidly, around 3 - 6 hours post VEGF inhibitor treatment. However, BMP signaling activation was not detected until 2 days following DOX-induced OE of two soluble VEGF receptors, whereas a marked downregulation of NANOG occurred within 1 day, even as early as 6 – 12 hours post-induction in the SS iOE cell line. The earlier downregulation of

NANOG relative to BMP signaling activation, coupled with the efficient rescue of VEGF signaling deficiency-induced phenotypes by *NANOG* OE, identifies NANOG as a key functional mediator downstream of the VEGF signaling pathway. Indeed, *NANOG* OE substantially diminished VEGF signaling deficiency-induced pSMAD1/5 activation as well as upregulation of BMP signaling components and key trophoblast genes, which underlies how NANOG suppresses BMP signaling activity and prevents trophoblast differentiation in hESCs. Of note, we showed that NANOG occupies regulatory elements of BMP pathway components and key trophoblast genes, arguing for a direct regulatory effect of NANOG on the transcription of these genes. On the other hand, *NANOG* OE also rescued VEGF signaling deficiency-induced downregulation of pluripotency-associated genes, suggesting a dual regulatory role for NANOG in sustaining pluripotency gene expression and repressing lineage specification-related pathways and genes. Intriguingly, we found that NANOG directly modulated *VEGFR2* expression in hESCs, revealing a positive feedback loop between NANOG and the VEGF signaling pathway to robustly safeguard hESC identity.

As a core pluripotency transcription factor, mechanisms by which NANOG expression is dynamically modulated have remained a key research focus in the stem cell field since its discovery. Previous studies showed that both TGF-β and bFGF could sustain NANOG expression in hESCs[19], although the underlying mechanism is not completely elucidated. TGF-β superfamily members (ACTIVIN A, NODAL and TGF-β) were reported to activate SMAD2/3, which directly enhanced NANOG expression[19]. The observation that NANOG OE bypassed the requirement for both TGF-β and FGF signaling in maintaining hESC self-renewal implies that these pathways act via the modulation of NANOG expression[19]. In this study, we uncovered that VEGF signaling pathway plays a critical role in sustaining *NANOG* expression in primed hESCs. Thus, NANOG likely functions as a central hub responding to various exogenous and endogenous signaling pathways to safeguard hESC identity. Nevertheless, it remains an

unresolved mystery how VEGF signaling orchestrates *NANOG* expression in hESCs. We sought to identify specific proteins mediating the regulatory effect of VEGF signaling on *NANOG* expression using proteomic and phosphoproteomic approaches. However, we failed to detect convincing substrate candidates. Thus, it remains unclear how VEGF signaling regulates *NANOG* expression in hESCs.

Although NANOG acts as a major effector downstream of VEGF signaling in hESCs, its OE failed to entirely abrogate VEGF pathway deficiency-induced BMP pathway activation, suggesting that there exist NANOG-independent mechanisms contributing to VEGF signaling-mediated suppression of BMP signaling activation. BMP4, which is known to induce trophoblast marker expression in hESCs, was reported to increase SMAD1 occupancy at the *NANOG* promoter, suggesting that BMP signaling could also regulate *NANOG* expression[19]. Here, we found that BMP pathway inhibition significantly suppressed VEGF signaling inactivation-induced morphological changes and upregulation of trophoblast genes. Therefore, suppression of BMP signaling accounts for, at least in part, the VEGF signaling-mediated inhibition of trophoblast-like lineage specification in primed hESCs. It remains unclear how VEGF signaling crosstalks with the BMP pathway in the context of hESC pluripotency maintenance and lineage specification.

Following embryo implantation in mammalian development, the trophectoderm (TE), arising from the outer cell layer of the blastocyst, gives rise to cytotrophoblasts (CTs), which can generate two differentiated cell types in human placenta, extravillous trophoblasts (EVTs) and syncytiotrophoblasts (STs). Human trophoblast stem cells (hTSCs) can be derived from the TE or first-trimester CTs, and can also be converted from hESCs. BMP4 has long been used to induce primed hESCs to differentiate into either the embryonic mesoderm or the extra-embryonic trophoblast, depending on the specific experimental conditions[34, 45-49]. However, in recent years, some researchers argued that primed hESCs-derived differentiated cells via the BAP or similar protocols exhibited features resembling the amnion rather than trophoblast cells[50, 51], unlike naive

hESCs, which can efficiently differentiate into trophoblasts. Indeed, the BMP pathway also plays a role in amnion development, which share many commonalities with trophoblasts. However, more recent works have challenged the notion of absolute lineage restriction in primed hPSCs. Several studies have showed that primed hESCs can generate trophoblast cells and hTSCs[40, 52-55]. For examples, the study by Wei et al. reported the successful generation of TSCs from primed hPSCs and demonstrated that BMP4 significantly enhanced this process[52]. Seetharam et al. revealed that primed hPSCs differentiated into placental trophoblasts, but not amnion cells, by BMP-directed differentiation protocols [40]. In the current study, we consider that VEGF signaling inhibition in primed hESCs could induce trophoblast-like differentiation, based on the following experimental evidence: i) differentiated cells derived from VEGFRi-treated hESCs displayed a uniform trophoblast-like morphology; ii) these cells exhibited lower levels of HLA-ABC, which is expressed in the amnion[56]; iii) they expressed human TE and CTB markers, such as *TROP2*, *GATA3*, *CDX2*, *TP63* and *ELF5*; iv) they had lower methylation levels in the *ELF5* promoter compared to undifferentiated hESCs; v) they could be induced to express marker genes of STB and EVT cells; vi) a set of amnion-specific genes, including *ACMSD*, *AQP9*, *CLDN22*, *TMEM174*, *MCCD1*, *HBA1*, and *SOX11*[40], were not upregulated in VEGF signaling deficiency-induced differentiated cells. Nevertheless, some VEGF signaling inhibition-upregulated genes such as *GATA2*, GATA3, *HAND1*, *TFAP2A*, and *KRT7* were also expressed in amnion cells. Moreover, there are differences in cell growth environments between our *in vitro* culture condition (mTeSR1) and the true *in vivo* developmental environment. Therefore, we do not rule out the possibility that trophoblast-like cells induced by the inactivation of the VEGF signaling pathway in primed hESCs may exhibit some characteristics of amnion cells.

Collectively, this study reveals an unexpected crucial role of endogenous VEGF signaling pathway as a guardian of human primed pluripotency. It clarifies how primed hESCs stabilize their undifferentiated state under basal conditions and provides a precise

molecular target for manipulating hESC fate. This enables controlled lineage specification, addressing a critical need in regenerative medicine and developmental biology research. The findings also inform the design of optimized protocols for hESC culture and directed differentiation, with relevance to disease modeling, tissue engineering, and cell-based therapies.

Methods

Ethics statement

All experiments were conducted in compliance with the ethical guidelines for the study of human embryonic stem cells issued jointly by the Chinese Ministry of Science and Technology and Ministry of Health in 2003 and adhered to relevant international regulations, including the 2021 ISSCR Guidelines for Stem Cell Research and Clinical Translation.

Reagents and resources

Reagents and resources are detailed in the Supplementary Information file as Supplementary Table 1.

Primed hESC culture and differentiation

The hESC line SHhES8 (Karyotype, 46, XX; derived in our lab)[29] was used in all experiments unless otherwise indicated. Primed SHhES8, H1 (Karyotype, 46, XY; WA01, WiCell), and H9 (Karyotype, 46, XX; WA09, WiCell) hESCs were routinely cultured in hESC-qualified Matrigel pre-coated plates in the mTeSR1 medium, and dissociated with Dispase every 4 to 5 days, unless otherwise indicated.

For differentiation in the E6 or RA medium, hESCs were dissociated with Accutase and replated (2 x 10^5 cells/well) onto Matrigel-coated 6-well plates in the TeSR-E6 or mTeSR1 with 1 μM RA for 2 to 4 days. For spontaneous EB formation, hESCs were dissociated by Dispase for about 15 min at 37°C and transferred to low attachment 60 mm dishes supplemented with the TeSR-E6 for 2 to 4 days.

For trophoblastic induction, hESCs were dissociated with Accutase and replated in the mTeSR1. On the next day, cells were adapted to radiation-inactivated mouse embryonic fibroblast (MEF, homemade)-conditioned medium (CM) containing 4 ng/mL bFGF. Twenty-four hours later, the medium was changed to the BAP medium[34] (E6 medium supplemented with 10 ng/mL BMP4, 1 μM ALK4/5/7 inhibitor A83-01 and 0.1 μM FGF2-signaling inhibitor PD173074) for 1 day. A summary of the experimental design is shown in Supplementary Fig. 3h. For EVT and ST differentiation induction, experiments were performed as previously described by Okae et al[39].

Naïve hESC culture

Naïve SHhES8 and H9 hESCs were converted from primed SHhES8 and H9 hESCs by the 5i/L/FA medium[30] , respectively, and cultured on MEF feeders. Naïve hESCs of both lines were cultured in the 5i/L/A medium, comprising a 1:1 mixture of DMEM/F12 and Neurobasal, 1% N2-supplement, 2% B27-Supplement, 2 mM L-GlutaMAX, 0.1 mM β-mercaptoethanol, 1 x MEM NEAA, 1 x penicillin-streptomycin, 1 μM PD0325901, 1 μM IM-12, 0.5 μM SB590885, 1 μM WH-4-023, 10 μM Y-27632, 20 ng/mL human LIF and 20 ng/mL Activin A. Cells were passaged every 4 days in a 1:2 to 1:3 split ratio after single-cell dissociation with Accutase.

All hESCs and their derivatives were cultured in a humidified incubator at 37°C with 21% O_2, 5% CO_2. Routine mycoplasma contamination tests were performed to ensure the absence of mycoplasma contamination.

Constructs

All constructs were validated by DNA sequencing.

pAAVS1-TRE3G-NANOG

For inducible overexpression (OE) of *NANOG* from the AAVS1 locus, its coding sequence was amplified by PCR from SHhES8 hESC complementary DNA (cDNA) using specific primers containing required restriction enzyme recognition sites (*NANOG* SalI F:

TAAAGTCGACATGAGTGTGGATCCAGCTTG and NANOG MluI R: ATGACGCGTTCACACGTCTTCAGGTTGCATG). The amplicon was subcloned into the pAAVS1-TRE3G-EGFP vector (a kind gift from Dr. Su-chun Zhang) to replace the original *EGFP* coding sequence, generating the plasmid pAAVS1-TRE3G-NANOG for derivation of *NANOG* iOE hESCs.

pROSA-Bsd-TRE3G-NANOG

For inducible *NANOG* OE from the ROSA26 locus, its coding sequence was amplified by PCR from SHhES8 hESC cDNA using specific primers (NANOG F2: ACGATGTTCCAGATTACGCTAGTGTGGATCCAGCTTGTCC and NANOG R2: GGCTAGCCATATGACGCGTCACACGTCTTCAGGTTGCA). The amplicon was subcloned into the pROSA-Bsd-TRE3G-3xFLAG-HA vector (homemade), generating the plasmid pROSA-Bsd-TRE3G-NANOG for derivation of SSN iOE hESCs.

pAAVS1-TRE3G-sFLT1-T2A-sKDR

For inducible OE of sFLT1 and sKDR, their coding sequences were respectively amplified by PCR from SHhES8 hESC cDNA using specific primers (TRE-sFLT1-F: CCTACCCTCGTAAAGTCGACATGGTCAGCTACTGGGACACCG; T2A-sFLT1-R: CACGTCACCGCATGTTAGAAGACTTCCCTCTGCCCTCTCCGCTGCCATGTTTTACAT TACTTTGTGTGGTA; T2A-sKDR-F: AGAGGAAGTCTTCTAACATGCGGTGACGTGGAGGAGAATCCCGGCCCTATGCAGA GCAAGGTGCGTGCTGG; SV40-sKDR-R: AGGCTAGCCATATGACGCGTTCACTCTGAGTCTTCTACAAGG). The two fragments were cloned into the pAAVS1-TRE3G-EGFP plasmid to replace the *EGFP* coding sequence, generating the pAAVS1-TRE3G-sFLT1-T2A-sKDR plasmid for derivation of SS iOE hESCs.

Treatment with inhibitors of growth factor receptors

Human ESCs were dissociated with Accutase and replated (5 x 10^5 cells/well) in Matrigel-

coated 6-well plates in the mTeSR1 supplemented with Y-27632 for 1 day. Subsequently, the medium was refreshed daily with the mTeSR1 supplemented with either 0.1% DMSO or individual inhibitors (2 μM Crenolanib, 5 μM Axitinib, 10 μM Erlotinib, 10 μM Tivozanib or 6 μM Lenvatinib) for the indicated durations.

Electroporation

Human ESCs were cultured in the mTeSR1 supplemented with Y-27632 (10 μM) for 2 hours prior to electroporation. Cells were dissociated into single cells using Accutase for 10 minutes at 37°C. A total of 3×10^6 cells were electroporated with appropriate combinations of plasmids in 100 μL of an electroporation solution (Mirus, MIR 50118) using the Lonza Nucleofector 2b device with program B-016 in 0.2 cm electroporation cuvettes.

Generation of the sFLT1/sKDR inducible overexpression (SS iOE) hESC line

SHhES8 hESCs were electroporated with a pair of single-guide RNA (sgRNA) plasmids (pX335-AAVS1-L and pX335-AAVS1-R[57]) and a donor plasmid (pAAVS1-TRE3G-sFLT1-T2A-sKDR), and selected using Puromycin (1 μg/mL) for 2 days. Surviving colonies were individually picked, expanded. The transcript levels were analyzed by real-time quantitative PCR (RT-qPCR) using primers specific for exogenous sFLT1 and sKDR (Ex-sFLT1 and Ex-sKDR) after treatment with doxycycline (DOX) for 2 days. Two clones, designated as SS iOE #7 and #10, respectively, were selected and expanded for further study. A control hESC line was parallelly generated by transfecting with an empty donor plasmid, referred to as Flag iOE. Sequences of the sgRNAs are listed in Supplementary Information file as Supplementary Table 2.

Generation of the *VEGFR1/2* inducible double knockout (*VEGFR1/2* dKO) hESC line

SHhES8 hESCs were electroporated with a pair of sgRNA plasmids (pX335-AAVS1-L and pX335-AAVS1-R) and a donor plasmid (pAAVS1-PDi-CRISPRn-VEGFR1/2-8xsgRNA), and selected using Blasticidin (5 μg/mL) for 3 days. Surviving colonies were individually

picked, expanded, and subjected to genomic DNA PCR analysis after doxycycline (0.5 μg/mL) treatment for 2 days. The primers used for PCR were as follows: *FLT1*-F (5'-GCTTCCCTTGGATCGGACTT-3'), *FLT1*-R (5'-GTCCTCTGGGAATGGGCTCT-3'), *KDR*-F (5'-CGCCGCAGAAAGTCCGTCT-3'), and *KDR*-R (5'-CTTTACGCAGGACAGTTGGCT-3'). Clones that exhibited inducible double knockout of *VEGFR1/2* were selected and expanded as the dKO hESC line for further study. In this single clone line, DOX treatment could lead to the simultaneous deletion of both *VEGFR1/2* as well as the soluble receptors *sFLT1* and *sKDR*. A negative control hESC line was generated following the identical electroporation, selection, and colony-picking workflow, but with a non-targeting EGFP-sgRNA[58, 59]. The related experiments were performed in the MEF-CM containing 4 ng/mL bFGF. Sequences of the sgRNAs are listed in Supplementary Information file as Supplementary Table 2.

Generation of *NANOG* inducible overexpression (*NANOG* iOE) hESC line

SHhES8 hESCs were electroporated with a pair of sgRNA plasmids (pX335-AAVS1-L and pX335-AAVS1-R) and a donor plasmid pAAVS1-TRE3G-NANOG. The transfected cells were selected using Puromycin (1 μg/mL) for 2 days. The surviving cells were expanded and validated by analyzing NANOG mRNA and protein levels. Sequences of the sgRNAs are listed in Supplementary Information file as Supplementary Table 2.

Generation of the sFLT1/sKDR and *NANOG* simultaneously inducible overexpression (SSN iOE) hESC line

SS iOE #10 hESCs were electroporated with a pair of sgRNA plasmids (pX335-ROSA26-L and pX335-ROSA26-R) and a donor plasmid pROSA26-TRE3G-*NANOG* and selected with Blasticidin (5 μg/mL) for 3 days. The surviving cells were expanded and validated by assessing NANOG mRNA and protein levels. Sequences of the sgRNAs used are listed in Supplementary Information file as Supplementary Table 2.

RNA extraction, cDNA synthesis and RT-qPCR

Total RNA was extracted from cells using the TRIzol reagent (Life Technologies, #15596026) according to the manufacturer's instruction. A total of 1.5 μg of RNA was reverse-transcribed into cDNA using the FastQuant RT Kit (TIANGEN, KR106) following the protocol provided by the manufacturer. RT-qPCR was performed on the ABI ViiA7 Real-Time PCR system using SYBR Premix Ex Taq II (Takara, #RR820L). *GAPDH* was used as an internal control to normalize expression levels of interested genes. Sequences of the primers used for RT-qPCR are listed in Supplementary Information file as Supplementary Table 3.

Western blot analysis

Cells were rinsed once with phosphate-buffered saline (PBS) and lysed in the RIPA buffer (50 mM Tris-HCl pH7.5, 150 mM NaCl, 0.1% SDS, 1% Nonidet P-40) supplemented with a protease inhibitor cocktail (PIC) and a phosphatase inhibitor cocktail (PPIC). The protein concentration was determined using the Pierce BCA Protein Assay Kit according to the manufacturer's instructions. Proteins were separated by 8% SDS-PAGE and transferred to 0.45 μm nitrocellulose membranes (GE Healthcare, #10600002). Membranes were blocked with 5% BSA in TBST (Tris-HCl buffered saline containing 0.1% Tween- 20; pH 7.4) for 1 hour at room temperature and then incubated with primary antibodies overnight at 4°C. The membranes were incubated with horseradish peroxidase (HRP)-conjugated secondary antibodies for 1 hour at room temperature. Chemiluminescent signals were detected using the SuperSignal West Pico Chemiluminescent Substrate.

To quantify the relative protein levels, the intensity of protein bands was measured using the ImageJ software. Subsequently, the ratio of the intensity between the interested protein band and the loading control band was calculated.

Immunofluorescence staining

The cells seeded on Matrigel-coated coverslips (Fisherbrand, #12-545-82) were fixed with 4% paraformaldehyde for 20 min at room temperature, washed 3 times with PBS, permeabilized with 0.2 % Triton X-100 in PBS for 20 min, and incubated in the blocking

buffer (3% BSA in PBS) for 1 hour at room temperature. The cells were then incubated with primary antibodies overnight at 4°C. On the next day, the cells were rinsed three times with PBS and incubated with secondary antibodies (FITC, 1:100; Cy3, 1:200) for 1 hour at room temperature. The nuclei were stained with DAPI (Sigma, #D9542). Images were captured using a Zeiss Cell Observer microscope.

RNA-seq and data analysis

Total RNA was extracted from cells using the TRIzol Reagent according to the manufacturer's instructions. RNA purification, reverse transcription, library construction and sequencing were performed by Annoroad Gene Technology Co., Ltd. (Beijing, China) or Shanghai Majorbio Bio-pharm Biotechnology Co., Ltd. (Shanghai, China) following the manufacturer's instructions (Illumina, San Diego, CA). The isolated RNA was enriched by Poly(A) tails and fragmented. A paired-end RNA-seq sequencing library was generated and sequenced using the HiSeq X Ten or NovaSeq Xplus sequencer with a read length of 2 × 150 bp. Levels of transcripts were calculated according to the fragments per kilobase of transcript per million mapped reads (FPKM) or the transcripts per million reads (TPM) method. Differentially expressed genes (DEGs) were identified using DESeq2[60] with the following criteria: $|\log_2 FC| \geqq 1$ and false discovery rate (FDR)-adjusted *p*-value < 0.05. Pathway and process enrichment analysis for DEGs was conducted using the Metascape (https://metascape.org/)[61]. The ontology sources included GO Biological Processes, KEGG Pathway, and Reactome Gene Sets. Terms with a *p*-value < 0.01, a minimum count of 3, and an enrichment factor > 1.5 were collected and grouped into clusters based on their membership similarities. The raw sequence data reported in this paper have been deposited in the Genome Sequence Archive in National Genomics Data Center, China National Center for Bioinformation / Beijing Institute of Genomics, Chinese Academy of Sciences (GSA-Human: HRA010308) that are publicly accessible at https://ngdc.cncb.ac.cn/gsa-human[62, 63].

ChIP-qPCR

Approximately 2 × 10^7 cells were cross-linked with 1% formaldehyde for 10 minutes and quenched with 0.125 M glycine for 5 minutes at room temperature. Cells were rinsed, scraped, and transferred into Eppendorf tubes containing cold PBS supplemented with PIC and PPIC, and then centrifuged to remove the supernatant. The cell pellet was suspended in 1 mL of 1% SDS FA cell lysis buffer (50 mM HEPES-KOH, pH 7.5, 150 mM NaCl, 1 mM EDTA, 1% Triton X-100, 0.1% sodium deoxycholate, and 1% SDS supplemented with PIC and PPIC). After rotating for 15 minutes at 4°C, the suspension was centrifuged at 15,000 × g for 30 minutes, and the supernatant was discarded. The pellet was resuspended in 1 mL of the 0.1% SDS FA cell lysis buffer. After rotating for 5 minutes at 4°C, the suspension was centrifuged at 15,000 × g for 30 minutes, and the supernatant was discarded. The pellet was resuspended in 1 mL of the 0.1% SDS FA cell lysis buffer and sonicated at 50% amplitude (30 seconds ON, 30 seconds OFF) for 2 minutes using a Sonics (UibraCELL) in ice water, followed by centrifugation at 15,000 × g for 10 minutes at 4°C. For the input sample, 50 µL of the supernatant was collected. For the immunoprecipitation, 900 µL of the supernatant was precleared and then incubated with 2.5 µg anti-NANOG antibody overnight at 4°C. On the next day, the reaction mixture was incubated with 100 µL Protein G Magnetic Beads (Millipore, LSKMAGG10) for 2 hours at 4°C, followed by gentle washing with the 0.1% SDS FA lysis buffer (3 times), high salt buffer (0.1% SDS FA cell lysis buffer with 350 mM NaCl), ChIP wash buffer (10 mM Tris-HCl, pH 8.0, 250 mM LiCl, 0.5% NP40, 0.5% sodium deoxycholate, 1 mM EDTA), and TE buffer (10 mM Tris-HCl, 1 mM EDTA, pH 8.0) sequentially. The chromatin was eluted from the beads with 200 µL of the ChIP elution buffer (50 mM Tris-HCl, 10 mM EDTA, 1% SDS, pH 7.5) for 30 minutes at 37°C. The input and eluted chromatin were decross-linked by adding 8 µL of 5 M NaCl and 1 µL RNase A (10 µg/µL) at 65°C for less than 16 hours, followed by adding 2 µL of 20 mg/mL protease K for 2 hours at 58°C. The resulting DNA was purified using a QIAquick PCR Purification Kit and quantified using a Quant-iT PicoGreen dsDNA Assay Kit. The purified DNA was

used for the examination of site-specific enrichments of NANOG. For RT-qPCR, 0.5 ng of the input or enriched DNA was used. Results were presented as the relative fold enrichment to the input. All primers used in ChIP-qPCR assays are listed in Supplementary Information file as Supplementary Table 4.

Flow cytometric analysis

Single-cell suspensions of hESCs were prepared through Accutase digestion. For surface marker detection, cells were incubated with the following antibodies at room temperature for 1 hour: FITC-conjugated HLA-ABC, PE-conjugated TROP2. After incubation, cells were washed three times with PBS. For GATA3 staining, cells were first fixed with 4% paraformaldehyde (PFA) in PBS for 15 minutes at room temperature, then permeabilized with 1.0% Triton X-100 in PBS for 15-20 minutes. Following blocking, cells were incubated with primary antibodies for 1 hour at room temperature, washed three times with PBS, and then incubated with a FITC-conjugated donkey anti-mouse secondary antibody (1:200 dilution) in the dark for 30 minutes. Cells were washed three times with PBS after secondary antibody incubation. Data were analyzed using the FlowJo software (version 10, Tree Star Inc.). The gating strategy is shown in Supplementary Fig. 7.

Promoter methylation characterization

The prediction of CpG islands in the promoter regions of *ELF5* was performed using the MethPrimer. Genomic DNA was processed according to the manufacturer's instructions of the EZ DNA Methylation-Gold™ Kit (ZYMO RESEARCH, #D5005). Following bisulfite treatment, unmethylated cytosines (C) in the genome were converted to uracils (U). Nested PCR amplification was then conducted using two pairs of primers specific to promoters of *ELF5,* sequentially. The amplified products were subsequently inserted into pGEM-T Easy vectors and sequenced to analyze the methylation status of these promoters. To quantify methylation levels of the promoter CpG islands, the sequenced files were uploaded to the Quantification tool for Methylation Analysis (QUMA:http://quma.cdb.riken.jp/). Primers used in the methylation PCR assay are listed

in Supplementary Information file as Supplementary Table 5.

Gene set enrichment analysis (GSEA)

The GSEA was performed to identify significant pathway activation patterns using the PID_BMP_PATHWAY gene set from the Pathway Interaction Database. Two separate comparisons were conducted: 1) VEGFR inhibitor (VEGFRi)-treated hESCs versus DMSO-treated hESCs, and 2) SS iOE +DOX hESCs versus SS iOE -DOX hESCs. The analysis was carried out using the GSEA software (version 4.3.2) with default parameters, including 1,000 permutations for significance testing, weighted enrichment statistic calculation, and signal-to-noise ratio as the ranking metric. Gene set permutations were selected as the permutation type to maintain the correlation structure among genes. Statistical significance of enrichments was evaluated by one-sided gene set permutation test with 1,000 iterations to generate the null distribution of enrichment scores (ES). Significant enrichment was defined with an FDR cutoff of 25% as recommended for discovery analyses, with nominal p-value < 0.05 considered supportive of enrichment signals. The normalized enrichment score (NES) was calculated to standardize the ES across gene sets with different sizes and correlation structures.

Statistics and Reproducibility

All experiments were designed with independent biological replicates, and each sample in the RT-qPCR assays included technical replicates. Numbers of biological replicates relevant for individual experiments are stated in figure legends. The unpaired two-tailed Student's t test was used for statistical tests of differences between two groups. For multiple comparison, The one-way ANOVA followed by Dunnett's post-hoc test was applied to assess differences relative to the control group. Data are shown as mean ± SEM. $p < 0.05$ was considered statistically significant (* $p < 0.05$, ** $p < 0.01$, and *** $p < 0.001$). All exact p values are provided in Source Data.

No statistical method was used to predetermine sample size. No data were excluded from the analyses. Cells were randomly allocated into experimental groups. The

investigators were not blinded to allocation during experiments and outcome assessment.

Data availability

RNA sequencing data were deposited in the Genome Sequence Archive in the National Genomics Data Center, Beijing Institute of Genomics (China National Center for Bioinformation) of the Chinese Academy of Sciences under accession code HRA010308 [https://ngdc.cncb.ac.cn/gsa-human/browse/HRA010308]. Source data are provided with this paper.

References

1. Thomson, J.A. *et al.* Embryonic Stem Cell Lines Derived from Human Blastocysts. *Science* **282**, 1145-1147 (1998).
2. Martin, G.R. Isolation of a pluripotent cell line from early mouse embryos cultured in medium conditioned by teratocarcinoma stem cells. *Proc. Natl. Acad. Sci.* **78**, 7634-7638 (1981).
3. Gilbert, J.M. *et al.* A controlled prospective trial of adjuvant razoxane in resectable colorectal cancer. *Recent Results Cancer Res* **79**, 48-58 (1981).
4. Nichols, J. & Smith, A. Naive and Primed Pluripotent States. *Cell Stem Cell* **4**, 487-492 (2009).
5. Brons, I.G.M. *et al.* Derivation of pluripotent epiblast stem cells from mammalian embryos. *Nature* **448**, 191-U197 (2007).
6. Rossant, J. Stem cells and early lineage development. *Cell* **132**, 527-531 (2008).
7. Boyer, L.A. *et al.* Core transcriptional regulatory circuitry in human embryonic stem cells. *Cell* **122**, 947-956 (2005).
8. Whyte, W.A. *et al.* Master Transcription Factors and Mediator Establish Super-Enhancers at Key Cell Identity Genes. *Cell* **153**, 307-319 (2013).
9. Suzuki, A. *et al.* Nanog binds to Smad1 and blocks bone morphogenetic protein-induced differentiation of embryonic stem cells. *P Natl Acad Sci USA* **103**, 10294-10299 (2006).
10. Hyslop, L. *et al.* Downregulation of NANOG induces differentiation of human embryonic stem cells to extraembryonic lineages. *Stem Cells* **23**, 1035-1043 (2005).
11. Vallier, L. *et al.* Activin/Nodal signalling maintains pluripotency by controlling Nanog expression. *Development* **136**, 1339-1349 (2009).
12. Wang, Z., Oron, E., Nelson, B., Razis, S. & Ivanova, N. Distinct lineage specification roles for NANOG, OCT4, and SOX2 in human embryonic stem cells. *Cell Stem Cell* **10**, 440-454 (2012).
13. Zaehres, H. *et al.* High-efficiency RNA interference in human embryonic stem cells. *Stem Cells* **23**, 299-305 (2005).
14. Fong, H.L., Hohenstein, K.A. & Donovan, P.J. Regulation of self-renewal and pluripotency by Sox2 in human embryonic stem cells. *Stem Cells* **26**, 1931-1938 (2008).
15. Bendall, S.C. *et al.* IGF and FGF cooperatively establish the regulatory stem cell niche of pluripotent human cells in vitro. *Nature* **448**, 1015-1021 (2007).

16. Beattie, G.M. *et al.* Activin A maintains pluripotency of human embryonic stem cells in the absence of feeder layers. *Stem Cells* **23**, 489-495 (2005).
17. Greber, B., Lehrach, H. & Adjaye, J. Fibroblast growth factor 2 modulates transforming growth factor β signaling in mouse embryonic fibroblasts and human ESCs (hESCs) to support hESC self-renewal. *Stem Cells* **25**, 455-464 (2007).
18. Levenstein, M.E. *et al.* Basic fibroblast growth factor support of human embryonic stem cell self-renewal. *Stem Cells* **24**, 568-574 (2006).
19. Xu, R.H. *et al.* NANOG is a direct target of TGFβ/Activin-mediated SMAD signaling in human ESCs. *Cell Stem Cell* **3**, 196-206 (2008).
20. Jiang, J.M. & Ng, H.H. TGFβ and SMADs talk to NANOG in human embryonic stem cells. *Cell Stem Cell* **3**, 127-128 (2008).
21. Kang, H.B. *et al.* Basic Fibroblast Growth Factor Activates ERK and Induces c-Fos in Human Embryonic Stem Cell Line MizhES1. *Stem Cells Dev.* **14**, 395-401 (2005).
22. Ho, L. *et al.* ELABELA Is an Endogenous Growth Factor that Sustains hESC Self-Renewal via the PI3K/AKT Pathway. *Cell Stem Cell* **17**, 435-447 (2015).
23. Apte, R.S., Chen, D.S. & Ferrara, N. VEGF in Signaling and Disease: Beyond Discovery and Development. *Cell* **176**, 1248-1264 (2019).
24. Patel, S.A. *et al.* Molecular Mechanisms and Future Implications of VEGF/VEGFR in Cancer Therapy. *Clin Cancer Res* **29**, 30-39 (2023).
25. Xin, C., Zhu, C., Jin, Y. & Li, H. Discovering the role of VEGF signaling pathway in mesendodermal induction of human embryonic stem cells. *Biochem Biophys Res Commun* **553**, 58-64 (2021).
26. Randolph, L.N., Bao, X., Oddo, M. & Lian, X.L. Sex-dependent VEGF expression underlies variations in human pluripotent stem cell to endothelial progenitor differentiation. *Sci. Rep.* **9**, 16696 (2019).
27. Zhao, H., Li, M., Ouyang, Q., Lin, G. & Hu, L. VEGF Promotes Endothelial Cell Differentiation from Human Embryonic Stem Cells Mainly Through PKC-ε/η Pathway. *Stem Cells Dev* **29**, 90-99 (2020).
28. Chen, G. *et al.* Blocking autocrine VEGF signaling by sunitinib, an anti-cancer drug, promotes embryonic stem cell self-renewal and somatic cell reprogramming. *Cell Res* **24**, 1121-1136 (2014).
29. Zhu, Z.X. *et al.* PHB Associates with the HIRA Complex to Control an Epigenetic-Metabolic Circuit in Human ESCs. *Cell Stem Cell* **20**, 274-+ (2017).
30. Theunissen, T.W. *et al.* Systematic identification of culture conditions for induction and maintenance of naive human pluripotency. *Cell Stem Cell* **15**, 471-487 (2014).
31. Fischer, L.A., Khan, S.A. & Theunissen, T.W. Induction of Human Naïve Pluripotency Using 5i/L/A Medium. *Methods Mol Biol* **2416**, 13-28 (2022).
32. Liu, Z.-L., Chen, H.-H., Zheng, L.-L., Sun, L.-P. & Shi, L. Angiogenic signaling pathways and anti-angiogenic therapy for cancer. *Signal Transduct Target Ther.* **8**, 198 (2023).
33. Mandegar, M.A. *et al.* CRISPR Interference Efficiently Induces Specific and Reversible Gene Silencing in Human iPSCs. *Cell Stem Cell* **18**, 541-553 (2016).
34. Amita, M. *et al.* Complete and unidirectional conversion of human embryonic stem cells to trophoblast by BMP4. *Proc Natl Acad Sci U S A* **110**, E1212-1221 (2013).
35. Shao, M. *et al.* NANOG governs cell metabolism and redox homeostasis in human naïve embryonic stem cells. *EMBO reports*, 1-33-33 (2025).

36. Ernst, J. & Kellis, M. ChromHMM: automating chromatin-state discovery and characterization. *Nat. Methods* **9**, 215-216 (2012).
37. Ernst, J. & Kellis, M. Chromatin-state discovery and genome annotation with ChromHMM. *Nature Protocols* **12**, 2478-2492 (2017).
38. Lee, C.Q.E. *et al.* What Is Trophoblast? A Combination of Criteria Define Human First-Trimester Trophoblast. *Stem Cell Rep* **6**, 257-272 (2016).
39. Okae, H. *et al.* Derivation of Human Trophoblast Stem Cells. *Cell Stem Cell* **22** (2018).
40. Seetharam, A.S. *et al.* The product of BMP-directed differentiation protocols for human primed pluripotent stem cells is placental trophoblast and not amnion. *Stem Cell Rep* **17**, 1289-1302 (2022).
41. Xiang, L. *et al.* A developmental landscape of 3D-cultured human pre-gastrulation embryos. *Nature* **577**, 537-542 (2020).
42. Bergmann, S. *et al.* Spatial profiling of early primate gastrulation in utero. *Nature* **609**, 136-143 (2022).
43. Li, J. *et al.* MEK/ERK signaling contributes to the maintenance of human embryonic stem cell self-renewal. *Differentiation* **75**, 299-307 (2007).
44. D'Amour, K.A. *et al.* Efficient differentiation of human embryonic stem cells to definitive endoderm. *Nat Biotechnol* **23**, 1534-1541 (2005).
45. Xu, R.H. *et al.* BMP4 initiates human embryonic stem cell differentiation to trophoblast. *Nat. Biotechnol.* **20**, 1261-1264 (2002).
46. Bernardo, A.S. *et al.* BRACHYURY and CDX2 mediate BMP-induced differentiation of human and mouse pluripotent stem cells into embryonic and extraembryonic lineages. *Cell Stem Cell* **9**, 144-155 (2011).
47. Yu, P.Z., Pan, G.J., Yu, J.Y. & Thomson, J.A. FGF2 Sustains NANOG and Switches the Outcome of BMP4-Induced Human Embryonic Stem Cell Differentiation. *Cell Stem Cell* **8**, 326-334 (2011).
48. Horii, M. *et al.* Human pluripotent stem cells as a model of trophoblast differentiation in both normal development and disease. *Proc Natl Acad Sci U S A* **113**, E3882-3891 (2016).
49. Roberts, R.M., Ezashi, T., Sheridan, M.A. & Yang, Y. Specification of trophoblast from embryonic stem cells exposed to BMP4. *Biol Reprod* **99**, 212-224 (2018).
50. Io, S. *et al.* Capturing human trophoblast development with naive pluripotent stem cells in vitro. *Cell Stem Cell* **28**, 1023-1039.e1013 (2021).
51. Guo, G. *et al.* Human naive epiblast cells possess unrestricted lineage potential. *Cell Stem Cell* **28**, 1040-+ (2021).
52. Wei, Y. *et al.* Efficient derivation of human trophoblast stem cells from primed pluripotent stem cells. *Sci Adv* **7** (2021).
53. Soncin, F. *et al.* Derivation of functional trophoblast stem cells from primed human pluripotent stem cells. *Stem Cell Rep* **17**, 1303-1317 (2022).
54. Jang, Y.J., Kim, M., Lee, B.K. & Kim, J. Induction of human trophoblast stem-like cells from primed pluripotent stem cells. *Proc Natl Acad Sci U S A* **119**, e2115709119 (2022).
55. Viukov, S. *et al.* Human primed and naïve PSCs are both able to differentiate into trophoblast stem cells. *Stem Cell Rep* **17**, 2484-2500 (2022).
56. Hammer, A. *et al.* Amnion epithelial cells, in contrast to trophoblast cells, express all classical HLA class I molecules together with HLA-G. *Am. J. Reprod. Immunol.* **37**, 161-171 (1997).

57. Fang, Z.Q. *et al.* SOX21 Ensures Rostral Forebrain Identity by Suppression of WNT8B during Neural Regionalization of Human Embryonic Stem Cells. *Stem Cell Rep* **13**, 1038-1052 (2019).
58. Doench, J.G. *et al.* Optimized sgRNA design to maximize activity and minimize off-target effects of CRISPR-Cas9. *Nat. Biotechnol.* **34**, 184-+ (2016).
59. Bertero, A. *et al.* Optimized inducible shRNA and CRISPR/Cas9 platforms for in vitro studies of human development using hPSCs. *Development* **143**, 4405-4418 (2016).
60. Love, M.I., Huber, W. & Anders, S. Moderated estimation of fold change and dispersion for RNA-seq data with DESeq2. *Genome Biol.* **15**, 550 (2014).
61. Zhou, Y. *et al.* Metascape provides a biologist-oriented resource for the analysis of systems-level datasets. *Nat Commun.* **10**, 1523 (2019).
62. Members, C.-N. & Partners Database Resources of the National Genomics Data Center, China National Center for Bioinformation in 2024. *Nucleic Acids Res.* **52**, D18-D32 (2024).
63. Chen, T. *et al.* The Genome Sequence Archive Family: Toward Explosive Data Growth and Diverse Data Types. *Genomics Proteomics Bioinformatics* **19**, 578-583 (2021).

Acknowledgements

We are grateful to Dr. Su-chun Zhang for generously providing the pAAVS1-TRE3G-EGFP plasmid. The working model was generated using BioRender. The study was supported by National Key R&D Program of China (2021YFA1100400 to Y.J., H.L. and L.L.), the Natural Science Foundation of Shanghai (19ZR1428300 to H.L.), and the Innovative Research Team of High-level Local Universities in Shanghai (SHSMU-ZLCX20210201 to Y.J.).

Authors contributions

H.L. and Y.J. conceived and designed the study and wrote the manuscript. X.W., C.W., and C.Z. performed the majority of the experiments and analyzed the results. H.L. assisted in conducting some key experiments and contributed to data analysis. H.J., Y.H., L.Y., M.S., and F.Z. conducted the bioinformatics analysis. C.X. and H.J. carried out the VEGFA165 iOE-related experiments. R.T. performed some western blot experiments. H.Z. and Q.W. helped to convert naïve hESCs from primed hESCs by the 5i/L/FA protocol. J.G. prepared radiation-inactivated MEFs. H.W. and B.L. established the NANOG iKD hESC line. Y.Z. helped with constructs. L.L. contributed to the design of the bioinformatics analysis. All authors reviewed and approved the final manuscript. Y.J. and H.L. supervised

the study.

Competing interests

The authors declare no competing interests.

Figure legends

Fig. 1: VEGF signaling components are highly expressed in primed hESCs.

a, Bright-field images of SHhES8 hESCs treated with DMSO (control), PDGFR inhibitor (PDGFRi: Crenolanib, 2 μM), VEGFR inhibitor (VEGFRi: Axitinib, 5 μM), and EGFR inhibitor (EGFRi: Erlotinib, 10 μM), respectively, for 2 days. Scale bars, 500 μm (top) and 100 μm (bottom).

b, RT-qPCR analysis results for relative mRNA levels of VEGF signaling ligands and receptors, pluripotency and lineage marker genes in SHhES8 hESCs cultured in the mTeSR1 self-renewal medium for 4 days or in the E6 differentiation medium for 2 days.

c, Representative immunofluorescence staining results for indicated proteins (red) in SHhES8 hESCs cultured in the mTeSR1 or E6 medium for 2 days. The nuclei were counterstained with DAPI (blue). Scale bars, 50 μm.

d, Bright-field images of SHhES8 and H9 hESCs cultured in the 5i/L/A medium (Naïve), mTeSR1 medium (Primed), and E6 differentiation medium (E6 D2), respectively. Scale bars, 100 μm.

e, RT-qPCR analysis results for relative mRNA levels of VEGF signaling ligands and receptors in SHhES8 (left) and H9 (right) hESCs cultured in the 5i/L/A medium (Naïve), mTeSR1 medium (Primed), respectively.

f, **g**, Representative western blot (**f**) and quantification (**g**) analysis results for relative protein levels of indicated proteins in SHhES8 and H9 hESCs cultured in the 5i/L/A medium (Naïve), mTeSR1 medium (Primed), and E6 differentiation medium (E6 D2), respectively.

Data in panels **b**, **e**, **g** are represented as mean ± SEM (n = 3 independent experiments). The unpaired two-tailed Student's *t* test was used. * $p < 0.05$, ** $p < 0.01$, and *** $p < 0.001$. For western blot analysis in panel **f**, α-Tubulin was used as a loading control. For microscope images in panels **a**, **c**, and **d**, three experiments were performed

independently with similar results. Source data are provided as a Source Data file.

Fig. 2: The VEGF pathway is essential for the maintenance of hESC Self-renewal.
a, Bright-field images of SHhES8 hESCs treated with DMSO (control), Tivozanib (Tiv), and Lenvatinib (Len), respectively, for 3 days. Scale bars, 100 μm.

b, **c**, Representative western blot (**b**) and quantification (**c**) analysis results for relative protein levels of pVEGFR1 (Y1213) and pVEGFR2 (Y951) in SHhES8 hESCs treated with DMSO, Tiv, and Len, respectively, for 3 days.

d, RT-qPCR analysis results for relative mRNA levels of pluripotency, trophoblast and three germ layer marker genes in SHhES8 hESCs treated with DMSO, Tiv, and Len, respectively, for the indicated time length.

e, RT-qPCR analysis results for relative mRNA levels of exogenous *sFLT1* (Ex-*sFLT1*) and *sKDR* (Ex-*sKDR*) in SS iOE #7 and SS iOE #10 hESCs cultured with or without DOX for 6 days.

f, **g**, Representative western blot (**f**) and quantification (**g**) analysis results for relative protein levels of pVEGFR1 (Y1213) and pVEGFR2 (Y951) in Flag iOE (the negative control), SS iOE #7, and SS iOE #10 hESCs cultured without or with DOX for 2 days.

h, Bright-field images of Flag iOE, SS iOE #7, and SS iOE #10 hESCs cultured without or with DOX for 6 days. Scale bars, 100 μm.

i, RT-qPCR analysis results for relative mRNA levels of marker genes of pluripotency, trophoblast and three germ layers in samples described in **h**.

Data in panels **c**, **e**, **g** and **i** are represented as mean ± SEM (n = 3 independent experiments). The unpaired two-tailed Student's *t* test was used. Data in the panel **d** are represented as mean ± SEM (n = 3 independent experiments). The one-way ANOVA followed by Dunnett's post-hoc test was used. * $p < 0.05$, ** $p < 0.01$, and *** $p < 0.001$. For western blot analyses in panels **b** and **f**, α-Tubulin was used as a loading control. For microscope images in panels **a** and **h**, three experiments were performed independently with similar results. Source data are provided as a Source Data file.

Fig. 3: The VEGF signaling pathway inhibits BMP signaling activity to prevent trophoblast specification.

a, **b**, The pathway and process enrichment analysis of Metascape for up-regulated differentially expressed genes (DEGs) in SHhES8 hESCs treated with VEGFR inhibitors (VEGFRi) for 3 days (**a**), or in SS iOE hESCs cultured with DOX for 6 days (**b**), based on our RNA-seq data.

c, **d**, The gene set enrichment analysis (GSEA) of the BMP pathway for up-regulated DEGs in SHhES8 hESCs treated with VEGFRi for 3 days, or in SS iOE hESCs cultured with DOX for 6 days, based on our RNA-seq data. Statistical significance of enrichments was evaluated by one-sided gene set permutation test with 1,000 iterations to generate the null distribution of enrichment scores (ES).

e, **f**, Representative western blot (**e**) and quantification (**f**) analysis results for relative protein levels of pSMAD1/5/8 and SMAD5 in SHhES8 hESCs treated with DMSO, Tiv, and Len, respectively, for the indicated durations.

g, **h**, Representative western blot (**g**) and quantification (**h**) analysis results for relative protein levels of pSMAD1/5/8 and SMAD5 in Flag iOE, SS iOE #7 and SS iOE #10 hESCs cultured under indicated conditions.

i, RT-qPCR analysis results for relative mRNA levels of pluripotency and trophoblast marker genes in SHhES8 hESCs treated with DMSO, Tiv, and Len, respectively, in the presence or absence of LDN-214117 (LDN) or DMH1 for 3 days.

j, RT-qPCR analysis results for relative mRNA levels of pluripotency and trophoblast marker genes in SS iOE #10 SHhES8 cultured under the indicated conditions.

Data in panels **i** and **j** are represented as mean ± SEM (n = 3 independent experiments). The unpaired two-tailed Student's *t* test was used. Data in panels **f** and **h** are represented as mean ± SEM (n = 3 independent experiments). The one-way ANOVA followed by Dunnett's post-hoc test was used. * $p < 0.05$, ** $p < 0.01$, and *** $p < 0.001$. For western blot analyses in panels **e** and **g**, α-Tubulin was used as a loading control. Source data

are provided as a Source Data file.

Fig. 4: NANOG acts as a key effector downstream of the VEGF signaling pathway.
a, **b**, The pathway and process enrichment analysis of Metascape for down-regulated DEGs in SHhES8 hESCs treated with VEGFR inhibitors (VEGFRi) for 3 days (**a**), or in SS iOE hESCs cultured with DOX for 6 days (**b**), based on our RNA-seq data.
c, **d**, Representative western blot (**c**) and quantification analysis results (**d**) for relative protein levels of NANOG and OCT4 in SHhES8 hESCs treated with DMSO, Tiv, and Len, respectively, for 3 days.
e, **f**, Representative western blot (**e**) and quantification analysis results (**f**) for relative protein levels of NANOG and OCT4 in Flag iOE, SS iOE #7, and SS iOE #10 hESCs cultured under the indicated conditions.
g, RT-qPCR analysis results for relative mRNA levels of pluripotency and trophoblast marker genes in NANOG iOE SHhES8 hESCs cultured under the indicated conditions for 4 days.
h, **i**, Representative western blot (**h**) and quantification analysis results (**i**) for relative protein levels of NANOG, pSMAD1/5/8, and SMAD5 in NANOG iOE and wildtype (WT) SHhES8 hESCs cultured under the indicated conditions.
j, RT-qPCR analysis results for relative mRNA levels of pluripotency and trophoblast marker genes in SS iOE #10 and SSN iOE hESCs cultured without or with DOX for 6 days.
k, **l**, Representative western blot (**k**) and quantification (**l**) analysis results for relative protein levels of NANOG, OCT4, pSMAD1/5/8, and SMAD5 in SS iOE #10 and SSN iOE hESCs cultured without or with DOX for 6 days. Ex-NANOG, ectopically expressed 3 x FLAG-HA-NANOG.
Data in panels **d**, **g**, **i**, **j** and **l** are represented as mean ± SEM (n = 3 independent experiments). The unpaired two-tailed Student's *t* test was used. Data in panel **f** are

represented as mean ± SEM (n = 3 independent experiments). The one-way ANOVA followed by Dunnett's post-hoc test was used. * $p < 0.05$, ** $p < 0.01$, and *** $p < 0.001$. For western blot analyses in panels **c**, **e**, **h** and **k**, α-Tubulin was used as a loading control. Source data are provided as a Source Data file.

Fig. 5: NANOG directly modulates the expression of important genes associated with the BMP pathway and trophoblast specification.

a, The heatmap showing Z-scores of 202 DEGs (VEGFRi vs DMSO) rescued by *NANOG* OE in NANOG iOE hESCs. The "up" and "down" were referred to as upregulated and downregulated DEGs induced by the VEGFR inhibitor treatment for 12 hours, and the "rescued" indicates the DEGs significantly rescued by *NANOG* OE. Some typical trophoblast, pluripotency and BMP pathway-related genes are shown on the right.

b, The heatmap showing Z-scores of 863 DEGs (with DOX vs without DOX in SS iOE cells) rescued by *NANOG* OE in SSN iOE hESCs at day 6. The "up" and "down" were referred to as DEGs induced by DOX treatment at day 6 in SS iOE cells, and the "rescued" indicates the DEGs significantly rescued by DOX treatment in SSN iOE cells. Two biological replicates (Rep.1 and Rep.2) were included for each group.

c, d, e, f, The pathway and process enrichment analysis of Metascape for down-regulated (**c**, **d**) or up-regulated (**e**, **f**) DEGs rescued by *NANOG* OE in NANOG iOE hESCs treated with VEGFRi for 12 hours (**c, e**), and in SSN iOE hESCs compared to SS iOE hESCs treated with DOX for 6 days (**d, f**), based on our RNA-seq data.

g, **h**, The ChIP-seq analysis result of NANOG binding at the promoter or enhancer sequences of BMP pathway genes (**g**) and trophoblast marker genes (**h**) in hESCs. Data were from NANOG ChIP-seq assays of our laboratory. The chromatin-state annotation track was produced from the ChromHMM based on ENCODE data. Promoter (red), promoter flanking (pink), enhancer (orange), weak enhancer (yellow), CTCF binding site (blue), transcribed (green), and repressed (gray).

i, **j**, ChIP-qPCR analysis results of NANOG binding at the promoter or enhancer of

selected genes described in **g** and **h**, respectively. Data are presented as means ± SEM relative to the input. n = 3 independent experiments. The unpaired two-tailed Student's *t* test was used. *$p < 0.05$, **$p < 0.01$ and ***$p < 0.001$. Source data are provided as a Source Data file.

Fig. 6: Suppression of the endogenous VEGF pathway triggers transition of primed hESCs from pluripotency to a trophoblast-like state.

a, Bright-field images of SHhES8 hESCs treated with Tiv or Len for 3 days. Scale bars, 100 μm.

b, Representative flow cytometric analysis results for the percentages of HLA-ABC$^+$, GATA3$^+$, or TROP2$^+$ cells in SHhES8 hESCs treated with DMSO or VEGFR inhibitors for 5 (HLA-ABC) or 3 (GATA3 and TROP2) days.

c, The statistical analysis result for the percentages of HLA-ABC$^+$, GATA3$^+$, or TROP2$^+$ cells described in **b**.

d, The bisulfite sequencing analysis result of genomic DNA methylation at the *ELF5* promoter in SHhES8 hESCs treated with DMSO or VEGFR inhibitors for 3 or 8 days. Solid circles depict methylated sites and open circles indicate unmethylated sites.

e, RT-qPCR analysis results for relative mRNA levels of marker genes associated with CT, EVT or ST cell types in SHhES8 hESCs treated with DMSO or VEGFR inhibitors for 3 days.

f, Representative immunofluorescence staining results of CDX2 (red), ELF5 (green), and TP63 (red) in SHhES8 hESCs treated with DMSO, Tiv, and Len, respectively, for 3 days. The nuclei were counterstained with DAPI (blue). Scale bars, 50 μm.

g, RT-qPCR analyses of relative mRNA levels for EVT or ST marker genes after Len-treated hESCs were induced to EVT or ST lineages for 8 or 6 days, respectively.

h, Heatmaps showing the expression of selected genes. Genes highly and specifically expressed in the amnion based on published data[40] are shown on the left. CT,

cytotrophoblast. The middle and right heatmaps show selected amnion-, trophoblast-, and pluripotency-marker genes in wild-type hESCs treated with the VEGF inhibitor (middle) and in SS iOE hESCs (right), respectively. Data (middle and right) are from our RNA-seq analysis.

Data in panels **c**, **e** and **g** are represented as mean ± SEM (n = 3 independent experiments). The unpaired two-tailed Student's *t* test was used. *$p < 0.05$, ** $p < 0.01$, and *** $p < 0.001$. For microscope images in panels **a** and **f**, three experiments were performed independently with similar results. Source data are provided as a Source Data file.

Fig. 7: A proposed working model for the function and underlying mechanisms of VEGF signaling in safeguarding human primed pluripotency.

In primed hESCs, endogenous VEGF signaling is active and essential for sustaining self-renewal and pluripotency. Mechanistically, VEGF signaling exerts dual regulatory effects: it represses the activity of the BMP pathway, a key driver of extra-embryonic lineage differentiation, while specifically activating the transcription of the core pluripotency factor NANOG. As a central "gatekeeper" of hESC identity, NANOG binds to the regulatory regions of a subset of BMP pathway components and trophoblast-associated genes, thereby suppressing their transcriptional activation and preventing inappropriate differentiation of hESCs into extra-embryonic lineages. Concurrently, NANOG maintains the expression of the VEGF receptor (e.g., VEGFR2/KDR) and critical pluripotency-associated genes, forming a feedforward regulatory loop that reinforces VEGF signaling activity and stabilizes the pluripotency state. Upon pharmacological or genetic inhibition of VEGF signaling, NANOG expression is rapidly downregulated, and the repressive constraint on the BMP pathway is relieved, leading to robust activation of BMP-mediated downstream signaling. This cascade of events ultimately results in the collapse of pluripotency and a cell fate switch toward extra-embryonic lineages. Created in

BioRender. Xu, Y. (2026) https://BioRender.com/gf39525.

Editor's Summary:

Both endogenous and exogenous signaling pathways are involved in the maintenance of self-renewal and pluripotency of human embryonic stem cells (hESCs). Here, the authors uncover that endogenous VEGF signaling safeguards pluripotency and prevents extra-embryonic differentiation in primed hESCs via activation of transcription factor NANOG and suppression of BMP signaling activity.

Peer review information: *Nature Communications* thanks Jacob Hanna and the other anonymous reviewer(s) for their contribution to the peer review of this work. A peer review file is available.

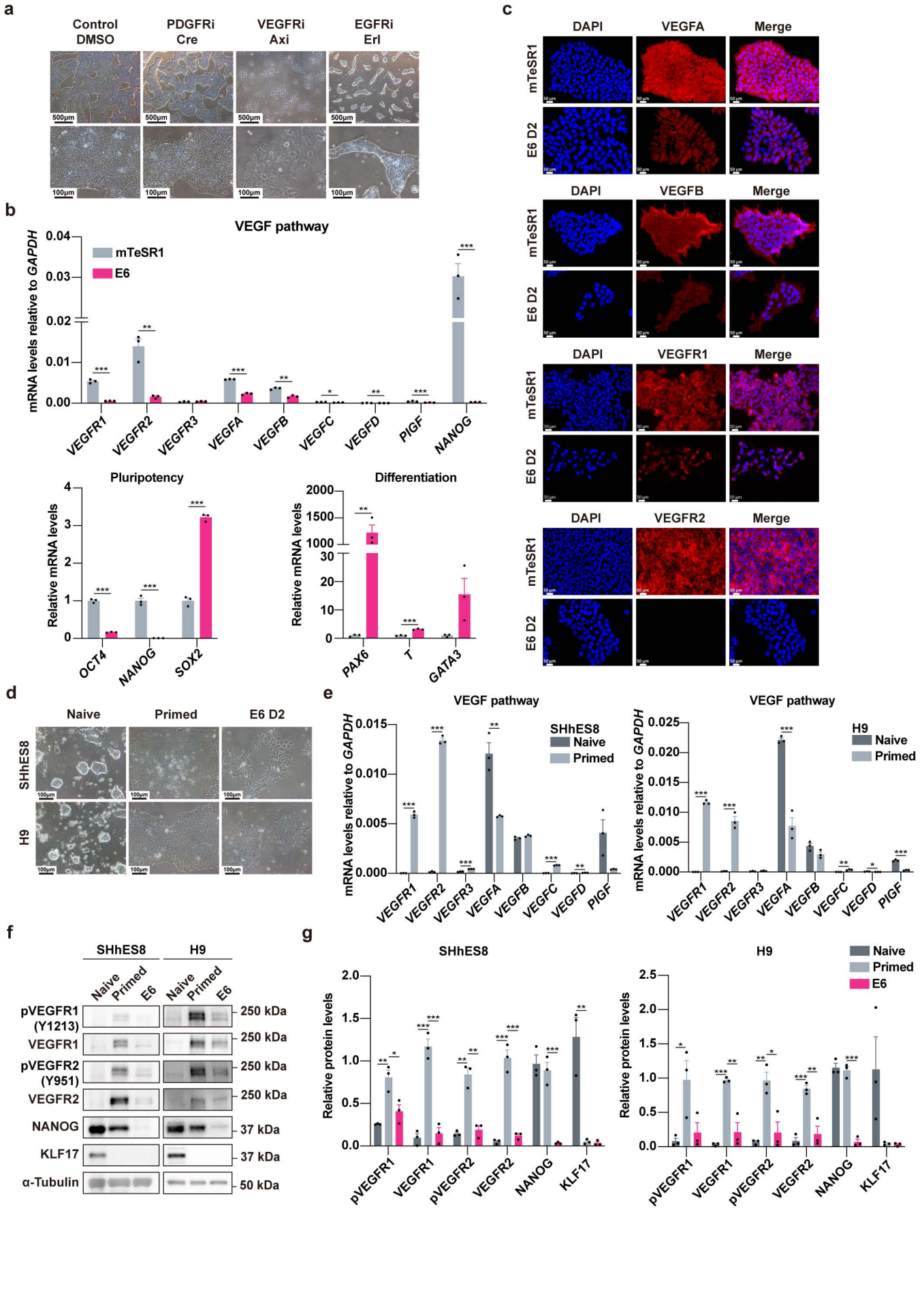
a
Control DMSO
PDGFRi Cre
VEGFRi Axi
EGFRi Erl
500µm
100µm
b
VEGF pathway
mRNA levels relative to GAPDH
mTeSR1
E6
VEGFR1
VEGFR2
VEGFR3
VEGFA
VEGFB
VEGFC
VEGFD
PIGF
NANOG
Pluripotency
Relative mRNA levels
OCT4
NANOG
SOX2
Differentiation
PAX6
T
GATA3
c
DAPI
VEGFA
VEGFB
VEGFR1
VEGFR2
Merge
mTeSR1
E6 D2
d
Naive
Primed
E6 D2
SHhES8
H9
e
VEGF pathway
SHhES8
H9
Naive
Primed
f
SHhES8
H9
Naive
Primed
E6
pVEGFR1 (Y1213)
VEGFR1
pVEGFR2 (Y951)
VEGFR2
NANOG
KLF17
α-Tubulin
250 kDa
37 kDa
50 kDa
g
SHhES8
H9
Relative protein levels
pVEGFR1
VEGFR1
pVEGFR2
VEGFR2
NANOG
KLF17

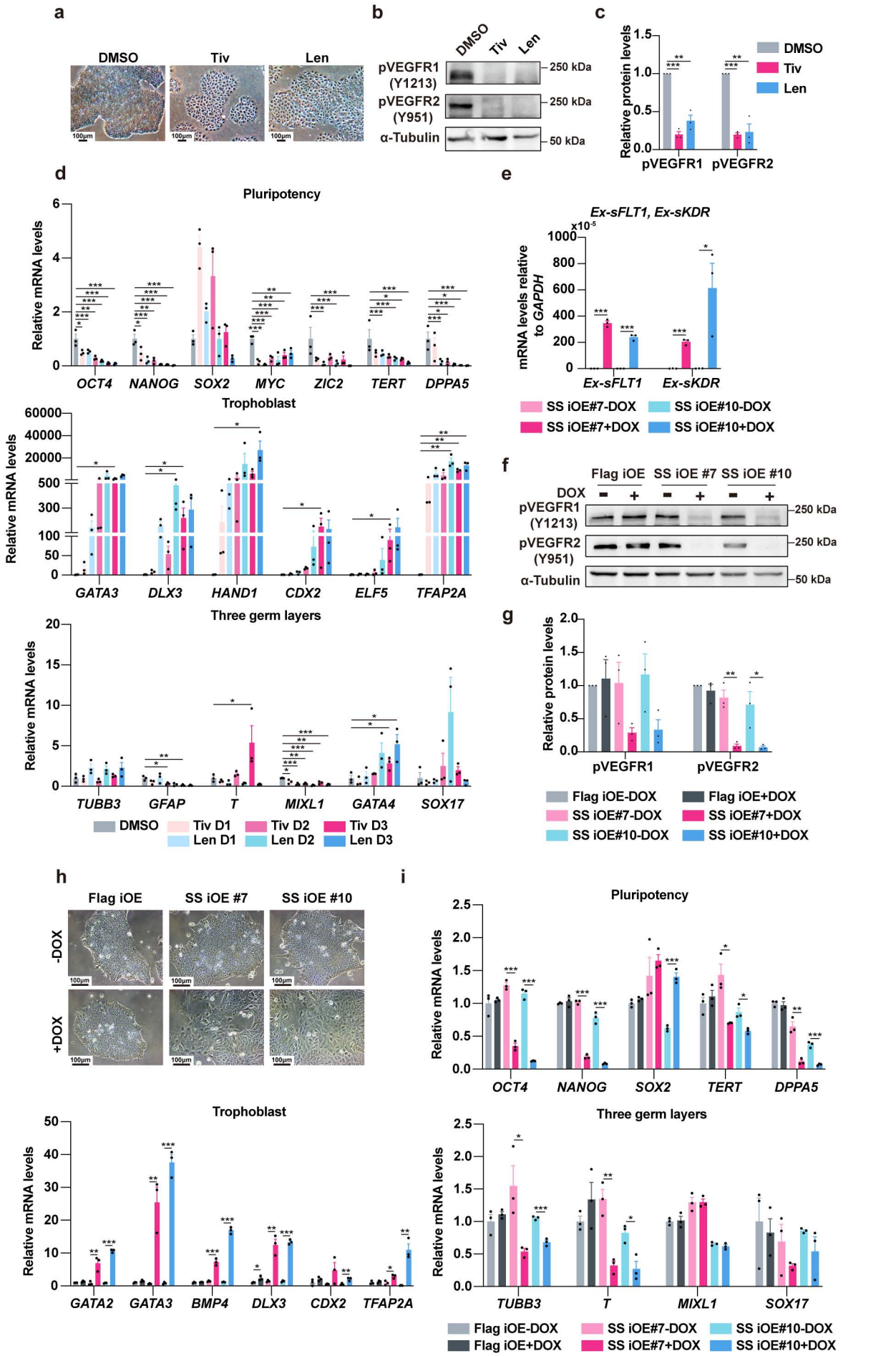
a
DMSO
Tiv
Len
100μm
b
DMSO
Tiv
Len
pVEGFR1 (Y1213)
pVEGFR2 (Y951)
α-Tubulin
250 kDa
250 kDa
50 kDa
c
Relative protein levels
DMSO
Tiv
Len
pVEGFR1
pVEGFR2
d
Pluripotency
Relative mRNA levels
OCT4
NANOG
SOX2
MYC
ZIC2
TERT
DPPA5
Trophoblast
GATA3
DLX3
HAND1
CDX2
ELF5
TFAP2A
Three germ layers
TUBB3
GFAP
T
MIXL1
GATA4
SOX17
DMSO
Tiv D1
Tiv D2
Tiv D3
Len D1
Len D2
Len D3
e
Ex-sFLT1, Ex-sKDR
mRNA levels relative to GAPDH
Ex-sFLT1
Ex-sKDR
SS iOE#7-DOX
SS iOE#7+DOX
SS iOE#10-DOX
SS iOE#10+DOX
f
Flag iOE
SS iOE #7
SS iOE #10
DOX
pVEGFR1 (Y1213)
pVEGFR2 (Y951)
α-Tubulin
250 kDa
250 kDa
50 kDa
g
Relative protein levels
pVEGFR1
pVEGFR2
Flag iOE-DOX
Flag iOE+DOX
SS iOE#7-DOX
SS iOE#7+DOX
SS iOE#10-DOX
SS iOE#10+DOX
h
Flag iOE
SS iOE #7
SS iOE #10
-DOX
+DOX
100μm
Trophoblast
Relative mRNA levels
GATA2
GATA3
BMP4
DLX3
CDX2
TFAP2A
i
Pluripotency
Relative mRNA levels
OCT4
NANOG
SOX2
TERT
DPPA5
Three germ layers
TUBB3
T
MIXL1
SOX17
Flag iOE-DOX
Flag iOE+DOX
SS iOE#7-DOX
SS iOE#7+DOX
SS iOE#10-DOX
SS iOE#10+DOX

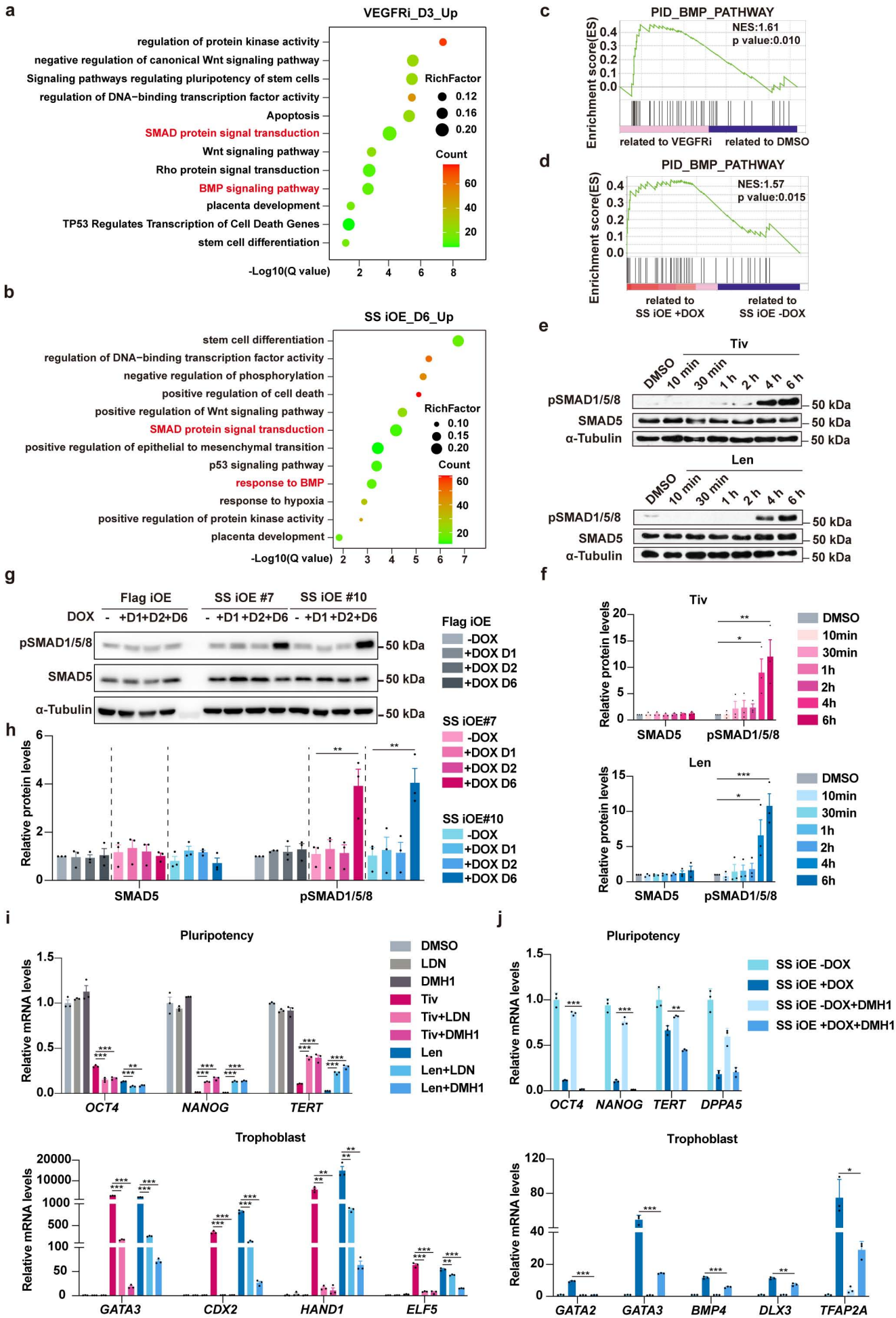
a
VEGFRi_D3_Up
regulation of protein kinase activity
negative regulation of canonical Wnt signaling pathway
Signaling pathways regulating pluripotency of stem cells
regulation of DNA−binding transcription factor activity
Apoptosis
SMAD protein signal transduction
Wnt signaling pathway
Rho protein signal transduction
BMP signaling pathway
placenta development
TP53 Regulates Transcription of Cell Death Genes
stem cell differentiation
-Log10(Q value)
RichFactor
Count
b
SS iOE_D6_Up
stem cell differentiation
regulation of DNA−binding transcription factor activity
negative regulation of phosphorylation
positive regulation of cell death
positive regulation of Wnt signaling pathway
SMAD protein signal transduction
positive regulation of epithelial to mesenchymal transition
p53 signaling pathway
response to BMP
response to hypoxia
positive regulation of protein kinase activity
placenta development
-Log10(Q value)
c
PID_BMP_PATHWAY
NES:1.61
p value:0.010
Enrichment score(ES)
related to VEGFRi
related to DMSO
d
PID_BMP_PATHWAY
NES:1.57
p value:0.015
Enrichment score(ES)
related to SS iOE +DOX
related to SS iOE -DOX
e
Tiv
DMSO
10 min
30 min
1 h
2 h
4 h
6 h
pSMAD1/5/8
SMAD5
α-Tubulin
50 kDa
Len
f
Tiv
Len
Relative protein levels
SMAD5
pSMAD1/5/8
DMSO
10min
30min
1h
2h
4h
6h
g
Flag iOE
SS iOE #7
SS iOE #10
DOX - +D1+D2+D6
pSMAD1/5/8
SMAD5
α-Tubulin
50 kDa
Flag iOE
-DOX
+DOX D1
+DOX D2
+DOX D6
SS iOE#7
SS iOE#10
h
Relative protein levels
SMAD5
pSMAD1/5/8
i
Pluripotency
Relative mRNA levels
OCT4
NANOG
TERT
DMSO
LDN
DMH1
Tiv
Tiv+LDN
Tiv+DMH1
Len
Len+LDN
Len+DMH1
Trophoblast
GATA3
CDX2
HAND1
ELF5
j
Pluripotency
SS iOE -DOX
SS iOE +DOX
SS iOE -DOX+DMH1
SS iOE +DOX+DMH1
OCT4
NANOG
TERT
DPPA5
Trophoblast
GATA2
GATA3
BMP4
DLX3
TFAP2A

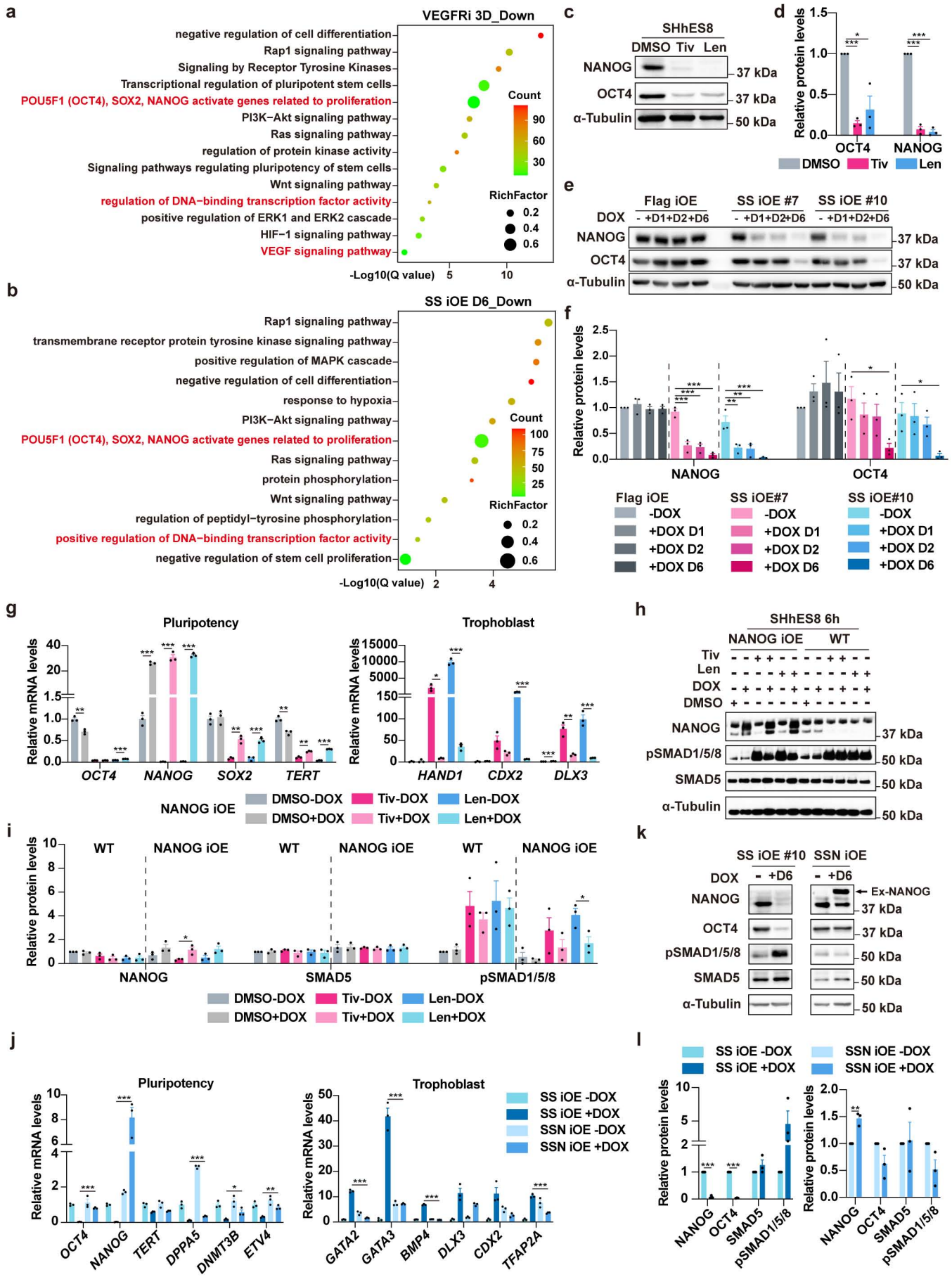
a
VEGFRi 3D_Down
negative regulation of cell differentiation
Rap1 signaling pathway
Signaling by Receptor Tyrosine Kinases
Transcriptional regulation of pluripotent stem cells
POU5F1 (OCT4), SOX2, NANOG activate genes related to proliferation
PI3K−Akt signaling pathway
Ras signaling pathway
regulation of protein kinase activity
Signaling pathways regulating pluripotency of stem cells
Wnt signaling pathway
regulation of DNA−binding transcription factor activity
positive regulation of ERK1 and ERK2 cascade
HIF−1 signaling pathway
VEGF signaling pathway
Count
90
60
30
RichFactor
0.2
0.4
0.6
-Log10(Q value) 5 10
b
SS iOE D6_Down
Rap1 signaling pathway
transmembrane receptor protein tyrosine kinase signaling pathway
positive regulation of MAPK cascade
negative regulation of cell differentiation
response to hypoxia
PI3K−Akt signaling pathway
POU5F1 (OCT4), SOX2, NANOG activate genes related to proliferation
Ras signaling pathway
protein phosphorylation
Wnt signaling pathway
regulation of peptidyl−tyrosine phosphorylation
positive regulation of DNA−binding transcription factor activity
negative regulation of stem cell proliferation
Count
100
75
50
25
RichFactor
0.2
0.4
0.6
-Log10(Q value) 2 4
c
SHhES8
DMSO Tiv Len
NANOG
OCT4
α-Tubulin
37 kDa
37 kDa
50 kDa
d
Relative protein levels
OCT4
NANOG
DMSO Tiv Len
e
Flag iOE
SS iOE #7
SS iOE #10
DOX
- +D1+D2+D6
NANOG
OCT4
α-Tubulin
37 kDa
37 kDa
50 kDa
f
Relative protein levels
NANOG
OCT4
Flag iOE
-DOX
+DOX D1
+DOX D2
+DOX D6
SS iOE#7
-DOX
+DOX D1
+DOX D2
+DOX D6
SS iOE#10
-DOX
+DOX D1
+DOX D2
+DOX D6
g
Pluripotency
Trophoblast
Relative mRNA levels
OCT4
NANOG
SOX2
TERT
HAND1
CDX2
DLX3
NANOG iOE
DMSO-DOX
DMSO+DOX
Tiv-DOX
Tiv+DOX
Len-DOX
Len+DOX
h
SHhES8 6h
NANOG iOE
WT
Tiv
Len
DOX
DMSO
NANOG
pSMAD1/5/8
SMAD5
α-Tubulin
37 kDa
50 kDa
50 kDa
50 kDa
i
WT
NANOG iOE
WT
NANOG iOE
WT
NANOG iOE
Relative protein levels
NANOG
SMAD5
pSMAD1/5/8
DMSO-DOX
DMSO+DOX
Tiv-DOX
Tiv+DOX
Len-DOX
Len+DOX
k
SS iOE #10
SSN iOE
DOX
- +D6
- +D6
NANOG
OCT4
pSMAD1/5/8
SMAD5
α-Tubulin
Ex-NANOG
37 kDa
37 kDa
50 kDa
50 kDa
50 kDa
j
Pluripotency
Trophoblast
Relative mRNA levels
OCT4
NANOG
TERT
DPPA5
DNMT3B
ETV4
GATA2
GATA3
BMP4
DLX3
CDX2
TFAP2A
SS iOE -DOX
SS iOE +DOX
SSN iOE -DOX
SSN iOE +DOX
l
SS iOE -DOX
SS iOE +DOX
SSN iOE -DOX
SSN iOE +DOX
Relative protein levels
NANOG
OCT4
SMAD5
pSMAD1/5/8
Relative protein levels
NANOG
OCT4
SMAD5
pSMAD1/5/8

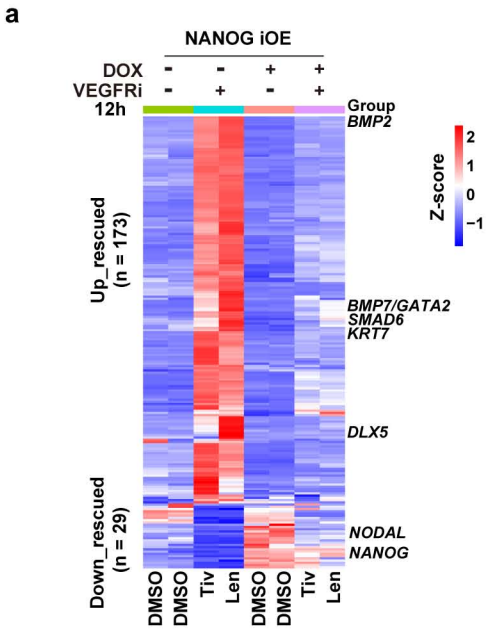
a
NANOG iOE
DOX
VEGFRi
12h
Group
BMP2
Z-score
Up_rescued (n = 173)
BMP7/GATA2
SMAD6
KRT7
DLX5
Down_rescued (n = 29)
NODAL
NANOG
DMSO
DMSO
Tiv
Len
DMSO
DMSO
Tiv
Len

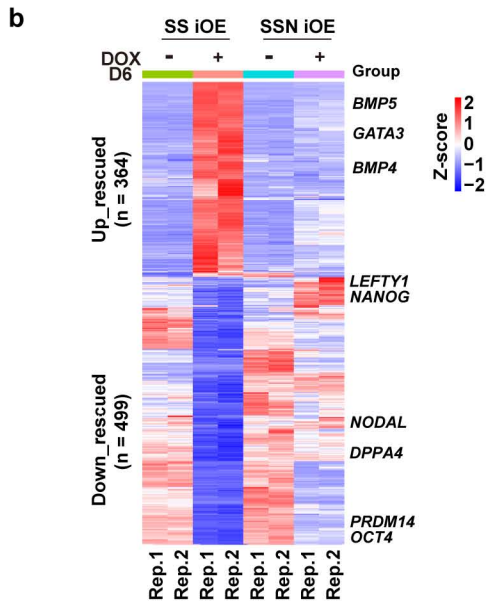
b
SS iOE
SSN iOE
DOX
D6
Group
BMP5
GATA3
BMP4
Z-score
Up_rescued (n = 364)
LEFTY1
NANOG
Down_rescued (n = 499)
NODAL
DPPA4
PRDM14
OCT4
Rep.1
Rep.2
Rep.1
Rep.2
Rep.1
Rep.2
Rep.1
Rep.2

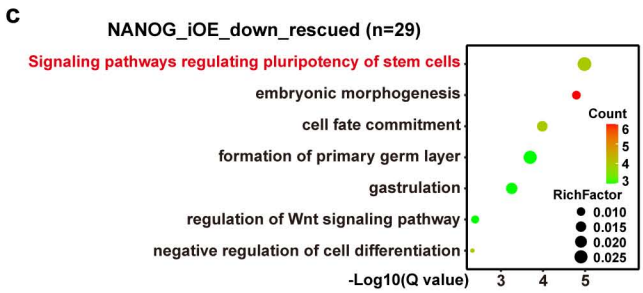
c
NANOG_iOE_down_rescued (n=29)
Signaling pathways regulating pluripotency of stem cells
embryonic morphogenesis
cell fate commitment
formation of primary germ layer
gastrulation
regulation of Wnt signaling pathway
negative regulation of cell differentiation
-Log10(Q value)
Count
RichFactor

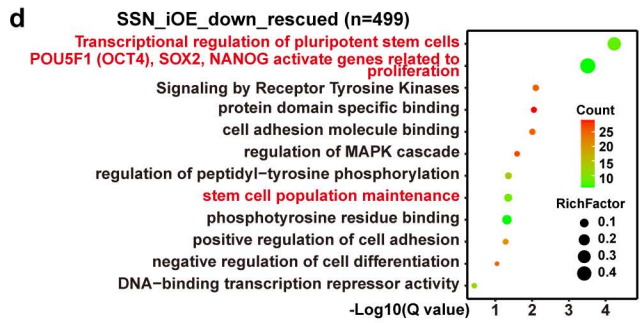
d
SSN_iOE_down_rescued (n=499)
Transcriptional regulation of pluripotent stem cells
POU5F1 (OCT4), SOX2, NANOG activate genes related to proliferation
Signaling by Receptor Tyrosine Kinases
protein domain specific binding
cell adhesion molecule binding
regulation of MAPK cascade
regulation of peptidyl−tyrosine phosphorylation
stem cell population maintenance
phosphotyrosine residue binding
positive regulation of cell adhesion
negative regulation of cell differentiation
DNA−binding transcription repressor activity
-Log10(Q value)
Count
RichFactor

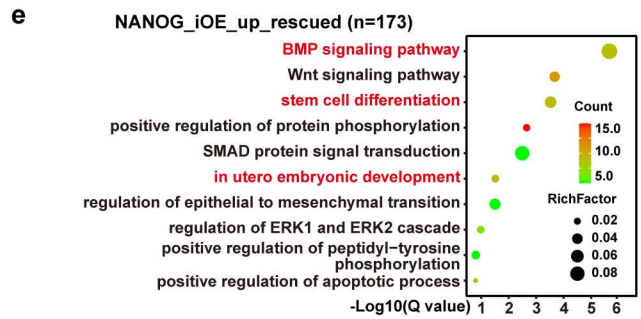
e
NANOG_iOE_up_rescued (n=173)
BMP signaling pathway
Wnt signaling pathway
stem cell differentiation
positive regulation of protein phosphorylation
SMAD protein signal transduction
in utero embryonic development
regulation of epithelial to mesenchymal transition
regulation of ERK1 and ERK2 cascade
positive regulation of peptidyl−tyrosine phosphorylation
positive regulation of apoptotic process
-Log10(Q value)
Count
RichFactor

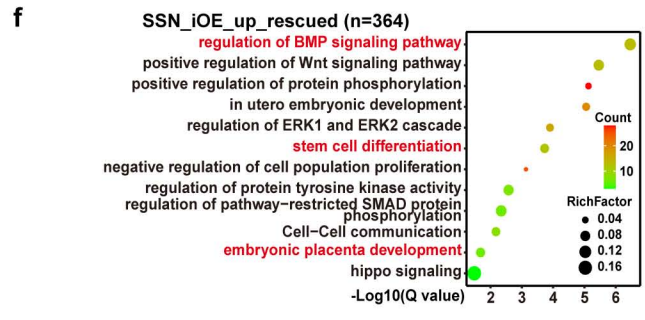
f
SSN_iOE_up_rescued (n=364)
regulation of BMP signaling pathway
positive regulation of Wnt signaling pathway
positive regulation of protein phosphorylation
in utero embryonic development
regulation of ERK1 and ERK2 cascade
stem cell differentiation
negative regulation of cell population proliferation
regulation of protein tyrosine kinase activity
regulation of pathway−restricted SMAD protein phosphorylation
Cell−Cell communication
embryonic placenta development
hippo signaling
-Log10(Q value)
Count
RichFactor

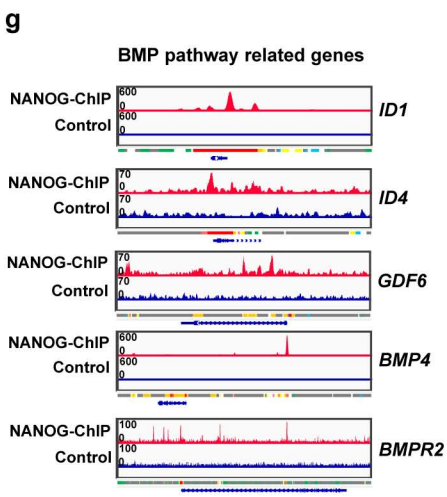
g
BMP pathway related genes
NANOG-ChIP
Control
ID1
ID4
GDF6
BMP4
BMPR2

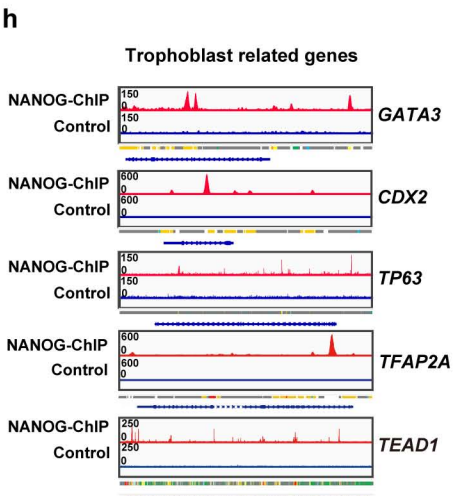
h
Trophoblast related genes
NANOG-ChIP
Control
GATA3
CDX2
TP63
TFAP2A
TEAD1

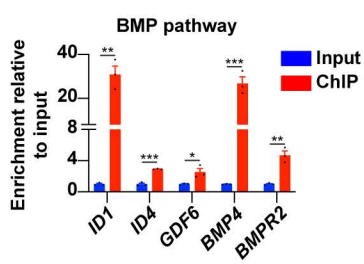
i
BMP pathway
Enrichment relative to input
Input
ChIP
ID1
ID4
GDF6
BMP4
BMPR2

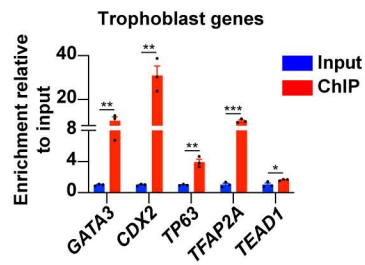
j
Trophoblast genes
Enrichment relative to input
Input
ChIP
GATA3
CDX2
TP63
TFAP2A
TEAD1

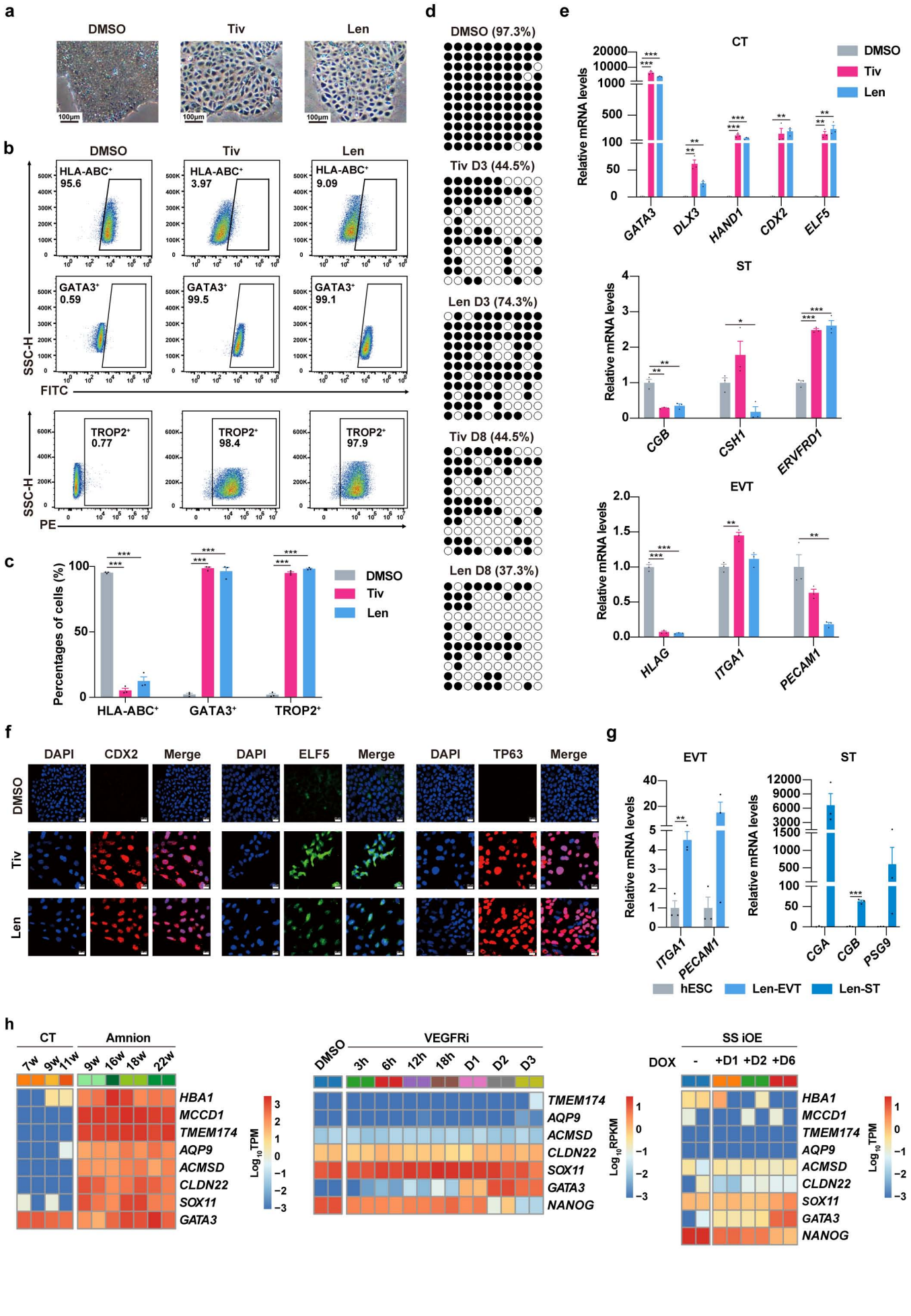
a
DMSO
Tiv
Len
100μm
b
HLA-ABC+ 95.6
HLA-ABC+ 3.97
HLA-ABC+ 9.09
GATA3+ 0.59
GATA3+ 99.5
GATA3+ 99.1
SSC-H
FITC
TROP2+ 0.77
TROP2+ 98.4
TROP2+ 97.9
PE
c
Percentages of cells (%)
HLA-ABC+
GATA3+
TROP2+
d
DMSO (97.3%)
Tiv D3 (44.5%)
Len D3 (74.3%)
Tiv D8 (44.5%)
Len D8 (37.3%)
e
CT
ST
EVT
Relative mRNA levels
GATA3
DLX3
HAND1
CDX2
ELF5
CGB
CSH1
ERVFRD1
HLAG
ITGA1
PECAM1
f
DAPI
CDX2
Merge
ELF5
TP63
g
EVT
ST
ITGA1
PECAM1
CGA
CGB
PSG9
hESC
Len-EVT
Len-ST
h
CT
Amnion
7w
9w
11w
16w
18w
22w
VEGFRi
DMSO
3h
6h
12h
18h
D1
D2
D3
SS iOE
DOX
+D1
+D2
+D6
HBA1
MCCD1
TMEM174
AQP9
ACMSD
CLDN22
SOX11
GATA3
NANOG
Log10TPM
Log10RPKM

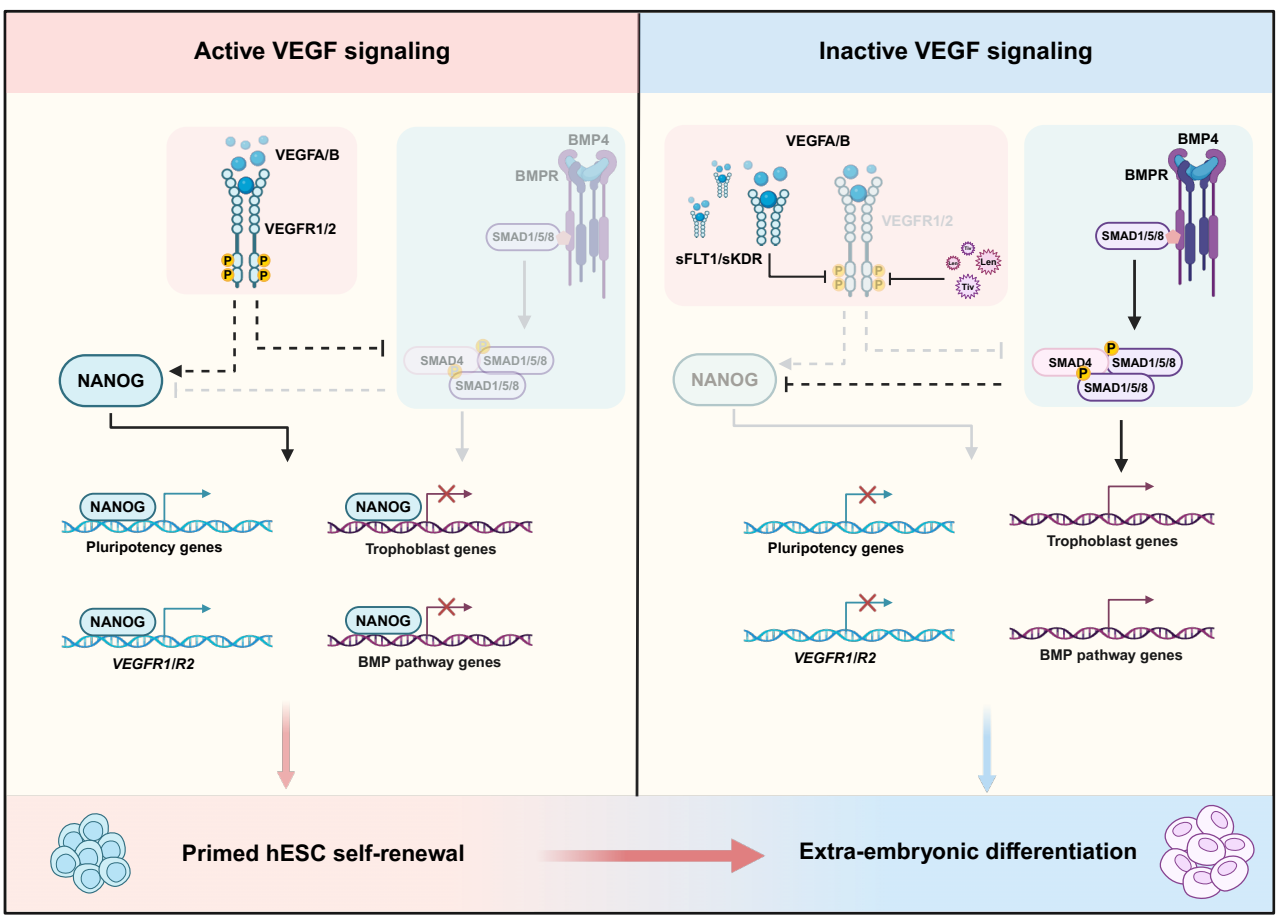
Active VEGF signaling
Inactive VEGF signaling
VEGFA/B
VEGFR1/2
BMP4
BMPR
SMAD1/5/8
SMAD4
NANOG
Pluripotency genes
Trophoblast genes
VEGFR1/R2
BMP pathway genes
sFLT1/sKDR
Len
Tiv
Primed hESC self-renewal
Extra-embryonic differentiation